ELSEVIER

Journal of Geometry and Physics 40 (2002) 320–369

JOURNAL OF GEOMETRY AND PHYSICS

www.elsevier.com/locate/jgp

On perturbed oscillators in 1–1–1 resonance: the case of axially symmetric cubic potentials

Sebastián Ferrer [a], Heinz Hanßmann [b], Jesús Palacián [c,*], Patricia Yanguas [c]

[a] *Departamento de Matemática Aplicada, Universidad de Murcia, 30071 Murcia, Spain*
[b] *Institut für Reine und Angewandte Mathematik der RWTH Aachen, 52056 Aachen, Germany*
[c] *Departamento de Matemática e Informática, Universidad Pública de Navarra, 31006 Pamplona, Spain*

Received 17 September 2000; received in revised form 9 April 2001

Abstract

Axially symmetric perturbations of the isotropic harmonic oscillator in three dimensions are studied. A normal form transformation introduces a second symmetry, after truncation. The reduction of the two symmetries leads to a one-degree-of-freedom system. To this end we use a special set of action–angle variables, as well as conveniently chosen generators of the ring of invariant functions. Both approaches are compared and their advantages and disadvantages are pointed out. The reduced flow of the normal form yields information on the original system.

We analyse the 2-parameter family of (arbitrary) axially symmetric cubic potentials. This family has rich dynamics, displaying all local bifurcations of co-dimension one. With the exception of six ratios of the parameter values, the dynamical behaviour close to the origin turns out to be completely determined by the normal form of order 1. We also lay the ground for a further study at the exceptional ratios.

MSC: 34C15; 34C20; 37G40; 70H08; 70H15; 70K50

Subj. Class.: Dynamical systems

Keywords: Genuine resonance; Axial symmetry; Normal forms; Reductions; Invariants; Relative equilibria; Periodic orbits; Invariant tori; Reconstruction of the flow

1. Introduction

One of the few methods that are available to study Hamiltonian systems is to find an integrable system that is close to it and to consider the former as a perturbation of the latter.

* Corresponding author. Tel.: +34-948-16-9554; fax: +34-948-16-9521.
E-mail address: palacian@unavarra.es (J. Palacián).

0393-0440/02/$ – see front matter
PII: S0393-0440(01)00041-9

In case the integrable system is non-degenerate, the flow of this system makes the phase space a *ramified torus bundle*. For instance, in three degrees of freedom the regular fibres of this bundle form 3-parameter families of invariant 3-tori, while 2-parameter families of invariant 2-tori, 1-parameter families of periodic orbits and isolated equilibria give rise to singular fibres. A perturbation of such a non-degenerate integrable system allows an immediate application of KAM-theory, cf. [6] and references therein. While resonant tori break up, most invariant tori survive the perturbation and are only slightly deformed. These are parametrised by large Cantor sets which are defined by Diophantine conditions on the frequencies.

Less can be said about perturbations of properly degenerate or *superintegrable* systems. In case that the perturbation "removes the degeneracy", KAM-theory is adapted in [3] to show that a measure-theoretically large part of the phase space becomes filled by maximal tori. Opposite to the non-degenerate case, where the geometry of the Cantor fibration into maximal tori is imposed by the unperturbed integrable system, the distribution of invariant tori in the perturbation of a superintegrable system is induced by the perturbation itself. If the integrable system is *minimally* superintegrable, having $(n+1)$-parameter families of invariant $(n-1)$-tori, a generic perturbation automatically "removes the degeneracy" and the surviving $(n-1)$-tori determine how the Cantor families of invariant n-torus are distributed in phase space, cf. [29,30,41].

For *maximally* superintegrable systems, like the Kepler system or the isotropic harmonic oscillator, it is more the exception than the rule that the perturbation "removes the degeneracy". However, systems perturbed from these are very important in applications. In fact, the more degenerate an integrable system is, the more non-integrable systems can be considered as a perturbation of that system. Taken to the extreme, every Hamilton function is a perturbation of the zero function (after an appropriate scaling of time).

It is a well-known phenomenon that Hamiltonian systems behave "more integrably" in the neighbourhood of their (elliptic) equilibria. In fact, after a scaling, the system can be considered as a perturbation of the linearisation at the equilibrium, an integrable system. In many cases it is possible to find another integrable approximation that is non-degenerate.

For instance, if there are no resonances of order ≤ 4 among the (normal) frequencies of the equilibrium, then the Birkhoff polynomial of degree 4 (in the original variables) will do, see [4]. The case of a single resonance of order 3 or 4 is studied in [37]. Here the Birkhoff normalising transformation leads to a normal form "with a resonance term" that defines again a non-degenerate integrable approximation.

In [28] frequency ratios of the form 1–2–k are considered, with $k = 2$ or $k \geq 5$, and also with $k = 1, 3, 4$ if the system has an appropriate discrete symmetry. In these cases the cubic normal form is integrable. The non-integrability of any normal form (other than the crude linear approximation) is proven in [17] for the 1–1–2 resonance, and in [35] a large step is made towards the same result for the 1–2–3 resonance.

The cubic terms in the normal form of the 1–1–1 resonance are zero, and the same holds true for the 1–1–3 resonance. This makes them "genuinely second-order resonances" (see [52] for the precise definition and a survey on genuinely first and second-order resonances). In fact, among the genuinely second-order resonances the 1–1–1 and the 1–1–3 are the most complicated: the normal form of order 4 contains, respectively, six and five terms.

These resonances have been used to model the motion in the central region of a galaxy (within a few core radii), cf. [51,55,59–61]. Both triaxial models and axially symmetric galaxies are under consideration. Most galaxies do not show a violent activity; more the contrary, they are supposed to exhibit a stationary behaviour. As a consequence of the observations made during the last two decades, astronomers conclude that many galactic components are neither spherical nor do they possess an axial symmetry, but they are triaxial objects, indeed. There is also an evidence of the triaxial structure of many galaxy bulges. Even barred galaxies evolve towards non-symmetric objects. Thus, the study of the dynamics of triaxial galaxies is a very interesting subject of research. Specifically, de Zeeuw and Merritt [62] suggest that most triaxial potentials are probably describable as Hamiltonian systems in 1–1–1 resonance. This fact has important implications for the existence of equilibrium triaxial galaxies. In other words, the analysis of the periodic orbits obtained as the equilibria of the reduced normalised system and their possible bifurcations is crucial to understand the behaviour of the galaxy.

This situation is similar in other fields of physics, such as molecular dynamics. Three-dimensional models based on perturbations of harmonic oscillators are adopted to describe the motion of the nuclei in a small molecule. Indeed, small-amplitude vibrations in molecules follow an oscillatory law, as their spectra and their reactions show, cf. [27].

We concentrate on the 1–1–1 resonance, and in this paper we assume the system to be axially symmetric, i.e. invariant under rotation about the vertical axis. In future work we hope to use the information we gain in this particular setting to attack the situation when the axial symmetry is broken, see also [24]. The axial symmetry immediately implies that the third component $N := x_1 p_2 - x_2 p_1$ of the angular momentum is an integral of motion. Furthermore, the periodic flow of the isotropic harmonic oscillator H_0 is used to put H_ε into normal form. As a consequence of the normalisation process, H_0 becomes a so-called "formal integral" of the normal form series. After truncation of the higher order terms, the normal form $\bar{H}_\varepsilon$ of order 2 defines an integrable approximation of H_ε (with integrals N and H_0).

Two methods have been proposed to deal with this kind of problems. In [20], following Deprit [15], the nodal-Lissajous variables (ℓ, g, ν, L, G, N) have been introduced (see also [21–23]). These are action–angle variables of the isotropic harmonic oscillator (in three degrees of freedom) that are particularly well adapted to the periodicity of the flow, in the same way as the Delaunay variables are for the Kepler problem. Borrowing some of the terminology of celestial mechanics, the fast variable ℓ is called the *elliptic anomaly* and varies for the isotropic harmonic oscillator $H_0 = \omega L$ as $\ell(t) = \omega t + \ell_0$. Moreover, as N and the modulus G of the angular momentum $x \times p$ are among the conjugate momenta, the effects of the perturbations on the unperturbed ellipses are rendered very intuitive in these variables. For instance, ν is a "slow" angle that measures the value of the *ascending node* of the orbital plane. In particular, the nodal-Lissajous variables allow to reduce the normal form $\bar{H}_\varepsilon$ to a one-degree-of-freedom problem since ν and ℓ are ignorable (cyclic) variables. The remaining variables g and G are co-ordinates of the (twice) reduced phase space, while N and L act as *distinguished* parameters.

Using singular reduction, in [12] the 2-torus symmetry is reduced by a set of generators $\tau_1, \tau_2, \tau_3, \tau_4$ of the ring of (smooth) invariant functions. For fixed values of $N = (1/2\omega)\tau_4$ and $L = (1/2\omega)(\tau_2 + \tau_3)$ this yields again a one-degree-of-freedom problem. For more

details see Section 2, where this reduction is detailed in two steps. Yanguas [58] performs the reductions in the opposite order. First, the invariants defined by the oscillator symmetry are used to express the normal form of an isotropic oscillator perturbed with arbitrary cubic terms (10 parameters, see also [24]). Then, the invariants $\tau_1, \tau_2, \tau_3, \tau_4$ are deduced as functions of the invariants of the oscillator symmetry. The twice reduced system is the same as the one obtained by using the procedure of [12]. As the perturbations considered in the present paper are axially symmetric themselves, it leads to sharper results to first reduce the axial symmetry and then perform the perturbation analysis in two degrees of freedom, and we will here exclusively consider the reductions in this order. However, we stress that for the non-symmetric 1–1–1 resonance the approach of [24,58] becomes crucial. See also the discussion of the Hamiltonian Hopf bifurcation in Section 4.5.

One of the goals of the present paper is to clarify the relation between the nodal-Lissajous variables and the singular reduction. We evaluate also the advantages and disadvantages of both approaches to symmetry reduction.

The Hamilton function H_ε we treat in this paper is a perturbation of the isotropic harmonic oscillator H_0 by a cubic potential. Because of the axial symmetry the most general expression is

$$H_\varepsilon(x, p) = \tfrac{1}{2}(p|p) + \tfrac{1}{2}\omega^2(x|x) + \varepsilon(\tfrac{1}{3}\alpha x_3^3 + \beta(x_1^2 + x_2^2)x_3), \tag{1}$$

where $(\cdot|\cdot)$ denotes the standard inner product. This defines a whole family of Hamiltonian systems. Let us discuss the role of the various parameters that occur. The frequency ω has physical dimensions time^{-1} and is the least important parameter; one of the reasons why we do not scale time to put $\omega = 1$ is that ω helps to distinguish between the energy H_0 and the momentum L. The dimensionless parameter ε expresses that we consider the cubic perturbation to be small. In fact ε can always be introduced by a scaling $x \mapsto \varepsilon x$, $p \mapsto \varepsilon p$, $H \mapsto \varepsilon^2 H$ and the form (1) of our Hamilton function then describes the dynamics close to the origin.

The parameters α and β are external parameters, the perturbing force field depends upon. Both have physical dimension length^{-1} time^{-2}. They are of order 1, e.g. $\alpha^2 + \beta^2 = 1$. It is important to make a clear distinction between the external parameters and the (internal or) distinguished parameters N and L. When dealing with the family of one-degree-of-freedom systems defined by $\bar{H}_\varepsilon$, one has to be careful about the type of transformation in parameter space one allows to make sure that the transformed N, L can still be interpreted as phase space variables.

In case $\beta = 0$ the system defined by (1) separates into the planar isotropic harmonic oscillator and a 1D cubic perturbation. Other parameter values where H_ε is known to be integrable are $\alpha = \beta$ and $\alpha = 6\beta$ (see [38] for a deduction of these choices to obtain integrable systems using Painlevé's criterion). Both correspond to axially symmetric 3D versions of two integrable systems in the plane. The first case, $\alpha = \beta$, is the extension of the system studied by Aizawa and Saitô [2]. The potential with $\alpha = 6\beta$ is the extension of the so-called Greene potential (see [19,50]). The cases $\beta = 0$ and $\alpha = \beta$ lead to degenerate normal forms $\bar{H}_\varepsilon$ as we will discuss in Section 4.5.

In this paper we study those regions of external parameters where the family of one-degree-of-freedom systems defined by $\bar{H}_\varepsilon$ (and parametrised by the distinguished parameters N and L) is structurally stable. The cubic terms in the normal form of (1) vanish and the

necessary second normalisation yields a quartic normal form. It turns out that there is only one non-integrable case where a higher order normal form is needed, the 3D Hénon–Heiles case $\alpha = -\beta$, cf. [33]. This case is dealt with in [21,22,58], which allows us to concentrate here on the quartic normal form $\bar{H}_\varepsilon$.

Since it is necessary to perform a second normalisation, additional terms $\varepsilon^2(\gamma_1(x_1^2 + x_2^2)^2 + \gamma_2(x_1^2 + x_2^2)x_3^2 + \gamma_3 x_3^4)$ would become equally important; a generic study of an axially symmetric Hamiltonian system in the neighbourhood of a 1–1–1 resonance thus involves all 5 parameters α, β, γ_1, γ_2, γ_3 (one of which is superfluous). Structural stability implies that the results we obtain for (1) also hold in a whole neighbourhood of the (α, β) plane in $(\alpha, \beta, \gamma_1, \gamma_2, \gamma_3)$ space. We will complete the study of the various regions in $(\alpha, \beta, \gamma_1, \gamma_2, \gamma_3)$ space in a subsequent paper.

This paper is organised as follows. In Section 2 we treat the various symmetries that occur. To this end we compare two approaches to the problem. The first leads to the construction of the nodal-Lissajous variables while the second approach is singular reduction. Only those properties that are needed in the sequel are stated, for a deeper study of the two approaches in their own right the reader is referred to, respectively, [20] and [12]. We end with a geometrical interpretation which explains the intimate relation between both results.

Section 3 contains the normalisation of the system (1). Again there are several approaches, one using the nodal-Lissajous variables, one performing the computation directly in the given co-ordinates and one using the invariants of the axial symmetry. We use all methods to calculate the second-order normal form and compare their advantages and disadvantages.

The normal form is analysed in Section 4 where we study the resulting one-degree-of-freedom problem. We obtain the (relative) equilibria and their bifurcations. In most cases the latter are versally unfolded by the distinguished parameters N and L. We give the different sectors of such structurally families within the (α, β)-space of external parameters.

Section 5 contains the perturbation analysis. First we reconstruct the dynamics of the normal form in two degrees of freedom. The original system (1) is axially symmetric itself and the perturbation analysis is carried out with this symmetry still reduced. Then the behaviour of the whole system in three degrees of freedom is reconstructed.

2. Singular reduction and action–angle variables

We perturb the harmonic oscillator with three equal frequencies. Therefore, we first recapitulate the main facts about this system. The presentation of these well-known results also allows us to fix notation. The reader may find more details in [25,36,40].

The *isotropic harmonic oscillator* in three degrees of freedom is the superposition of three harmonic oscillators with the same frequency ω. The energy reads

$$H_0(x, p) = \tfrac{1}{2}(p|p) + \tfrac{1}{2}\omega^2(x|x)$$

and the resulting flow on the phase space $T^*\mathbb{R}^3 \cong \mathbb{R}^3 \times \mathbb{R}^3$ is periodic. In particular, the isotropic harmonic oscillator is a maximally superintegrable Hamiltonian system.

The invariance of H_0 under the group $SO(3)$ of rotations implies that the angular momentum vector $x \times p$ is kept fixed by the flow. Since H_0 is even invariant under the larger

group $U(3)$ of unitary complex 3×3 matrices, there are more integrals of motion. They form the tensor $(p_j p_k + \omega^2 x_j x_k)_{j,k=1,2,3}$ which can be thought of as a generalisation of the Laplace or Runge–Lenz vector, see [34]. This tensor determines the ellipse in configuration space along which the flow proceeds. Indeed, the angular momentum is an eigenvector with eigenvalue 0, and the other two eigenvalues $\omega L \pm \omega\sqrt{L^2 - G^2}$ are related to the semi-major and semi-minor axes of the ellipse. Here $G = \|x \times p\|$ denotes the modulus of the angular momentum and ωL stands for the energy H_0.

2.1. The axial symmetry

The cubic perturbations $H_\varepsilon = H_0 + \varepsilon(\frac{1}{3}\alpha x_3^3 + \beta(x_1^2 + x_2^2)x_3)$ of the isotropic harmonic oscillator that we consider are invariant under the axial S^1-action

$$\begin{aligned} \varrho: \quad S^1 \times T^*\mathbb{R}^3 &\to T^*\mathbb{R}^3, \\ (\nu, (x, p)) &\mapsto (\exp_\nu x, \exp_\nu p), \end{aligned}$$

where $\exp_\nu$ stands for the rotation

$$\exp \begin{pmatrix} 0 & -\nu & 0 \\ \nu & 0 & 0 \\ 0 & 0 & 0 \end{pmatrix} = \begin{pmatrix} \cos\nu & -\sin\nu & 0 \\ \sin\nu & \cos\nu & 0 \\ 0 & 0 & 1 \end{pmatrix}$$

about the third axis. From Noether's theorem, or by direct verification, one concludes that the third component $N = x_1 p_2 - x_2 p_1$ of the angular momentum is an integral of motion. We use this symmetry to simplify the analysis of the given (axially symmetric) Hamiltonian system. In fact we compare two different ways to accomplish this goal.

To define the nodal-Lissajous variables we have to assume that the total angular momentum G does not vanish. This allows us to choose the angular momentum vector $x \times p$ as third co-ordinate axis. In the new co-ordinates the motion in configuration space takes place in the $(\tilde{x}_1, \tilde{x}_2)$-plane, in particular we have $G = \tilde{x}_1\tilde{p}_2 - \tilde{x}_2\tilde{p}_1$. The Whittaker transformation

$$\begin{aligned} \mathcal{W}: \quad \{(x, p) \in T^*\mathbb{R}^3 \,||N| < G\} &\to T^*\mathbb{R}^2 \times T^*S^1, \\ (x_1, x_2, x_3, p_1, p_2, p_3) &\mapsto (\tilde{x}_1, \tilde{x}_2, \tilde{p}_1, \tilde{p}_2, \nu, N) \end{aligned}$$

suits our needs, see [56, Chapter 13, p. 343], and also [14]. Writing $\cos I = N/G$, $0 < I < \pi$, we have

$$\begin{aligned} &x_1 = \tilde{x}_1 \cos\nu - \tilde{x}_2 \sin\nu \cos I, \quad x_2 = \tilde{x}_1 \sin\nu + \tilde{x}_2 \cos\nu \cos I, \quad x_3 = \tilde{x}_2 \sin I, \\ &p_1 = \tilde{p}_1 \cos\nu - \tilde{p}_2 \sin\nu \cos I, \quad p_2 = \tilde{p}_1 \sin\nu + \tilde{p}_2 \cos\nu \cos I, \quad p_3 = \tilde{p}_2 \sin I. \end{aligned} \tag{2}$$

The angle ν determines the nodal line, i.e. ν measures the angle from the x_1 axis to the intersection between the old (x_1, x_2) plane and the new $(\tilde{x}_1, \tilde{x}_2)$ plane. Thus, I is the angle between the two planes. The condition $|N| < G$ ensures that $x \times p$ is not already parallel to the x_3 axis, so ν is well defined.

The Whittaker transformation is a (homogeneous) canonical transformation, i.e. the symplectic structure remains the standard one. In the new co-ordinates our Hamilton function

reads

$$H_\varepsilon(\tilde{x},\tilde{p},\nu,N)=\frac{1}{2}(\tilde{p}_1^2+\tilde{p}_2^2)+\frac{\omega^2}{2}(\tilde{x}_1^2+\tilde{x}_2^2)$$
$$+\varepsilon\sqrt{1-\frac{N^2}{(\tilde{x}_1\tilde{p}_2-\tilde{x}_2\tilde{p}_1)^2}}\left(\frac{\alpha}{3}\left(1-\frac{N^2}{(\tilde{x}_1\tilde{p}_2-\tilde{x}_2\tilde{p}_1)^2}\right)\tilde{x}_2^3\right.$$
$$\left.+\beta\left(\tilde{x}_1^2\tilde{x}_2+\frac{N^2}{(\tilde{x}_1\tilde{p}_2-\tilde{x}_2\tilde{p}_1)^2}\tilde{x}_2^3\right)\right).$$

By construction ν is a cyclic variable, thus the conjugate momentum N acts as a (distinguished) parameter of the system. For a fixed value a of N we have reduced to a two-degree-of-freedom system. In particular, the flow of the isotropic harmonic oscillator becomes $\varphi_t(\tilde{x},\tilde{p},\nu,N)=(\tilde{x}\cos\omega t+(1/\omega)\tilde{p}\sin\omega t,-\omega\tilde{x}\sin\omega t+\tilde{p}\cos\omega t,\nu,N)$.

The Whittaker transformation is only defined on the (open and dense) set where $|N|<G$. A global way to reduce the axial symmetry is to use a set of generators of the Poisson algebra of (smooth) ϱ-invariant functions, cf. [11]. In the present situation a suitable choice is

$$\sigma_1=z_1^2+z_2^2,\qquad \sigma_2=z_1\bar{z}_1+z_2\bar{z}_2+\bar{z}_1z_2-z_1\bar{z}_2,\qquad \sigma_3=z_3, \tag{3}$$

where

$$z_j=\omega x_j+\mathrm{i}p_j,\quad j=1,2,3, \tag{4}$$

see [12] for more details. These generators are constrained by the relations $P(\sigma):=\sigma_1\bar{\sigma}_1-(\mathrm{Re}\,\sigma_2)^2+(\mathrm{Im}\,\sigma_2)^2=0$ and $\mathrm{Re}\,\sigma_2\geq 0$. Eqs. (3) induce a Poisson bracket on $\mathbb{C}^3\cong\mathbb{R}^6$ which has two *Casimir elements*, functions that commute with all other functions: the relation P and the third component $N(\sigma)=(1/2\omega)\mathrm{Im}\,\sigma_2$ of the angular momentum. This implies that our realisation $P^{-1}(0)$ of the reduced phase space $T^*\mathbb{R}^3/S^1$ is invariant under every Hamiltonian system on $\mathbb{C}^3$, and that the level sets $\{N=a\}$ are invariant subsets. On these 4D subvarieties the Poisson bracket is non-degenerate, giving rise to a symplectic structure.

We have again reduced to two degrees of freedom. The subset $|N|=G$ which we had to exclude for the Whittaker transformation gets reduced to

$$\{\sigma\in\mathbb{C}^3|P(\sigma)=0,\sigma_3\,\mathrm{Re}\,\sigma_2=\sigma_1\bar{\sigma}_3\}$$

and contains in particular the plane $\{(0,0,\sigma_3)|\sigma_3\in\mathbb{C}\}$. This follows directly from (9), using the definition (6a) and (6b). At that plane the reduced phase space $P^{-1}(0)$ is not smooth, but has a cone-like singularity. Our Hamilton function gets reduced to

$$H_\varepsilon(\sigma)=\frac{1}{2}\mathrm{Re}\,\sigma_2+\frac{1}{2}\sigma_3\bar{\sigma}_3+\varepsilon\left(\frac{\alpha}{3\omega^3}(\mathrm{Re}\,\sigma_3)^3+\frac{\beta}{2\omega^3}(\mathrm{Re}\,\sigma_1+\mathrm{Re}\,\sigma_2)\mathrm{Re}\,\sigma_3\right)$$

and the flow of the isotropic harmonic oscillator becomes $\varphi_t(\sigma)=(\mathrm{e}^{-2\mathrm{i}\omega t}\sigma_1,\sigma_2,\mathrm{e}^{-\mathrm{i}\omega t}\sigma_3)$.

2.2. The oscillator symmetry

The flow φ_t of the unperturbed system X_{H_0} defines the S^1-action ψ as

$$\begin{aligned}\psi: \quad & S^1 \times T^*\mathbb{R}^3 \quad \to \quad T^*\mathbb{R}^3,\\ & (\ell, (x, p)) \quad \mapsto \quad \varphi_{\ell/\omega}(x, p),\end{aligned}$$

which we call the *oscillator symmetry*. Our perturbed Hamilton function H_ε is not invariant under this action, but we normalise it in Section 3 and the resulting normal form does have this oscillator symmetry. Again we compare the two ways to incorporate this symmetry. In fact, both the invariants σ_j and the nodal-Lissajous variables we now obtain may be used to perform the normalisation.

By construction the unperturbed system has become in Whittaker co-ordinates the planar isotropic harmonic oscillator, parametrised by (ν, N). In particular, the oscillator symmetry reads

$$\begin{aligned}\psi: \quad & S^1 \times (T^*\mathbb{R}^2 \times T^*S^1) \quad \to \quad T^*\mathbb{R}^2 \times T^*S^1,\\ & (\ell, (\tilde{x}, \tilde{p}, \nu, N)) \qquad \mapsto \quad \left(\begin{pmatrix} (\cos \ell t) I_2 & \frac{1}{\omega}(\sin \ell t) I_2 \\ -\omega(\sin \ell t) I_2 & (\cos \ell t) I_2 \end{pmatrix} \begin{pmatrix} \tilde{x} \\ \tilde{p} \end{pmatrix}, \nu, N\right),\end{aligned}$$

where $I_2 = \begin{pmatrix} 1 & 0 \\ 0 & 1 \end{pmatrix}$ denotes the identity. From Noether's theorem, or by direct verification, one concludes that every oscillatory symmetric Hamiltonian system has $L = (1/2\omega)(\tilde{p}|\tilde{p}) + (\omega/2)(\tilde{x}|\tilde{x})$ as an integral of motion. In a second step we now use the Lissajous transformation

$$\begin{aligned}\mathcal{L}: \quad & \{(\tilde{x}, \tilde{p}) \in T^*\mathbb{R}^2 | G < L\} \times T^*S^1 \quad \to \quad T^*\mathbb{T}^3,\\ & (\tilde{x}_1, \tilde{x}_2, \tilde{p}_1, \tilde{p}_2, \nu, N) \qquad\qquad \mapsto \quad (\ell, g, \nu, L, G, N)\end{aligned}$$

introduced in [15]. Writing $\tilde{s} = \sqrt{(L+G)/(2\omega)}$ and $\tilde{d} = \sqrt{(L-G)/(2\omega)}$, we have

$$\begin{aligned}\tilde{x}_1 &= \tilde{s}\cos(g+\ell) - \tilde{d}\cos(g-\ell), \quad \tilde{p}_1 = -\omega(\tilde{s}\sin(g+\ell) + \tilde{d}\sin(g-\ell)),\\ \tilde{x}_2 &= \tilde{s}\sin(g+\ell) - \tilde{d}\sin(g-\ell), \quad \tilde{p}_2 = \omega(\tilde{s}\cos(g+\ell) + \tilde{d}\cos(g-\ell)).\end{aligned} \tag{5}$$

The angle ℓ describes the position on an ellipse in configuration space, measured from the semi-minor axis. This makes ℓ the elliptic anomaly, see [15]. The other variables define the ellipse, which is centred at the origin. The angle g gives the position of the semi-minor axis reckoning from the $\tilde{x}_1$ axis, i.e. from the nodal line. The eccentricity

$$\tilde{e} = \frac{2\sqrt{\tilde{s}\tilde{d}}}{\tilde{s}+\tilde{d}} = \sqrt{\frac{2\sqrt{L^2-G^2}}{L+\sqrt{L^2-G^2}}}$$

of the ellipse determines its shape, while the size is encoded in the length

$$\tilde{s} - \tilde{d} = \sqrt{\frac{1}{\omega}(L - \sqrt{L^2-G^2})}$$

of the semi-minor axis. The condition $G < L$ ensures that the ellipse does not degenerate to a circle, thus g and ℓ are well defined. Finally ν still represents the angle of the ascending node of the orbital plane, the inclination of which is given by $\cos I = N/G$.

The nodal-Lissajous transformation $\mathcal{L} \circ \mathcal{W}$ is obtained explicitly combining the Eqs. (2) and (5). Thus, the nodal-Lissajous variables are defined on

$$\{(x, p) \in T^*\mathbb{R}^3 | |N| < G < L\}.$$

For completeness we give here other state functions that we use later: $\eta = G/L, e^2 = 1-\eta^2$, $c = N/G$, $s^2 = 1 - c^2$ and $\mu = N/L$. These state functions prove indispensable when working with the normal form $\bar{H}_\varepsilon$ of H_ε in nodal-Lissajous variables in an efficient way.

The Hamilton function of the isotropic harmonic oscillator now reads $H_0 = \omega L$ and yields the equations of motion

$$\dot{\ell} = \omega, \qquad \dot{g} = 0, \qquad \dot{\nu} = 0, \qquad \dot{L} = 0, \qquad \dot{G} = 0, \qquad \dot{N} = 0.$$

Thus, the elliptic anomaly ℓ is a linear function of time, describing the position of the particle on the trajectory. The projection of this trajectory into configuration space is exactly the ellipse fixed by (g, ν, L, G, N). In particular, invariants like the tensor $(p_j p_k + \omega^2 x_j x_k)_{j,k=1,2,3}$ or the angular momentum vector $x \times p$ can be expressed in terms of (g, ν, L, G, N), see [20]. The nodal-Lissajous variables are action–angle variables of the isotropic harmonic oscillator that are particularly well suited in that they immediately reflect the periodic character of the flow. In the terminology of Nehorošev [47] they are generalised action–angle variables. Note, however, that these variables yield a 2:1 covering because (ℓ, g, ν, L, G, N) and $(\ell-\pi, g+\pi, \nu, L, G, N)$ represent the same point in $T^*\mathbb{R}^3$, see [15,20].

On the (first) reduced phase space, i.e. expressed in the invariants $\sigma_1, \sigma_2, \sigma_3$, the oscillator symmetry reads

$$\begin{array}{rccl} \psi: & S^1 \times \mathbb{C}^3 & \to & \mathbb{C}^3, \\ & (\ell, \sigma) & \mapsto & (\mathrm{e}^{-2\mathrm{i}\ell}\sigma_1, \sigma_2, \mathrm{e}^{-\mathrm{i}\ell}\sigma_3) \end{array}$$

and its generator becomes $L(\sigma) = (1/2\omega)(\mathrm{Re}\,\sigma_2 + \sigma_3\bar{\sigma}_3)$. Again we follow Cushman et al. [12] in the choice of a set of generators of the Poisson algebra of (smooth) ψ-invariant functions to reduce the symmetry. The complex-valued function

$$\tau_1 = \sigma_1\bar{\sigma}_3^2 \tag{6a}$$

and the real-valued functions

$$\tau_2 = \mathrm{Re}\,\sigma_2, \qquad \tau_3 = \sigma_3\bar{\sigma}_3, \qquad \tau_4 = \mathrm{Im}\,\sigma_2, \qquad \tau_5 = \sigma_1\bar{\sigma}_1 \tag{6b}$$

are constrained by the relations $\tau_1\bar{\tau}_1 = \tau_3^2\tau_5$, $\tau_3 \geq 0$. Since we are only interested in the subset

$$\{\tau \in \mathbb{C} \times \mathbb{R}^4 | P(\tau) = 0\},$$

we may use $P(\tau) = \tau_5 - \tau_2^2 + \tau_4^2$ to eliminate τ_5, see [12] for more details. Combining (3) with (6a) and (6b) we thus have reduced the phase space $T^*\mathbb{R}^3$ to

$$V = \{\tau \in \mathbb{C} \times \mathbb{R}^3 | R(\tau) = 0, \tau_3 \geq 0\},$$

where $R(\tau) = \tau_1\bar{\tau}_1 - \tau_3^2(\tau_2^2 - \tau_4^2)$. Next to R there are two more Casimir elements of the reduced Poisson bracket on $\mathbb{C} \times \mathbb{R}^3$. The third component $N(\tau) = (1/2\omega)\tau_4$ of the angular momentum is inherited from the first reduction, while $L(\tau) = (1/2\omega)(\tau_2 + \tau_3)$ is made a Casimir element by the second reduction. In particular $H_0 = \omega L$ defines the zero vector field on the second reduced phase space V, the flow of the isotropic harmonic oscillator having been completely reduced.

Fixing values a of N and b of L we obtain 2D subvarieties that are invariant under every Hamiltonian system on the second reduced phase space. Eliminating $\tau_4 = 2\omega a$ and $\tau_3 = 2\omega b - \tau_2$ these become

$$V_{a,b} = \{\tau \in \mathbb{C} \times \mathbb{R} || \tau_1| = \sqrt{F_{a,b}(\tau_2)}, 2\omega|a| \leq \tau_2 \leq 2\omega b\},$$

where

$$F_{a,b}(\tau_2) = (\tau_2 - 2\omega b)^2(\tau_2^2 - 4\omega^2 a^2);$$

the relation R has now turned into $R_{a,b}(\tau) = (\mathrm{Re}\,\tau_1)^2 + (\mathrm{Im}\,\tau_1)^2 - F_{a,b}(\tau_2)$. For $|a| < b$ the twice reduced phase space $V_{a,b}$ is a topological sphere that has conical singularities at

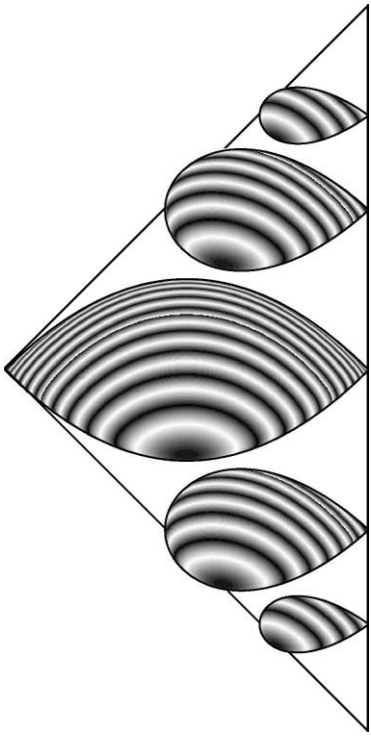

Fig. 1. Different slices $N^{-1}(a) \cap L^{-1}(b) \cong V_{a,b}$ of the second reduced phase space $V = \{\tau \in \mathbb{C} \times \mathbb{R}^3 | R(\tau) = 0, \tau_3 \geq 0\}$. For $0 < |a| < b$ these have the form of a turnip, while $V_{0,b}$ has a second singularity and looks like a lemon. On each slice the flow defined by the Hamilton function $H = G$ is depicted, giving an impression of the local charts (γ, Γ) defined below.

$\tau = (0, 2\omega b)$ and (for $a = 0$) also at $\tau = (0, 0)$. This gives $V_{a,b}$ the shape of a turnip if $a \neq 0$, and $V_{0,b}$ looks like a lemon, cf. Fig. 1. The Poisson structure on $V_{a,b}$ can be written as the vector triple product,

$$\{f, h\} = 2\omega(\nabla f \times \nabla h | \nabla R_{a,b}). \tag{7}$$

Outside the singular points this gives rise to a symplectic structure on $V_{a,b}$.

The points on the second reduced phase space V represent S^1-families of ellipses, which get transformed into each other by the axial S^1-action ϱ. Whenever non-trivial rotations ϱ_ν fix an ellipse — also preserving its orientation — this leads to a singular point on V. Indeed, this is equivalent to the 2-torus action

$$\begin{array}{rccl} \psi \circ \varrho: & (S^1 \times S^1) \times T^*\mathbb{R}^3 & \to & T^*\mathbb{R}^3, \\ & ((\nu, \ell), z) & \mapsto & \varrho_\nu(\psi_\ell(z)) \end{array}$$

having a non-trivial isotropy group. In this way the equatorial circular ellipses get reduced to singular points $V_{\pm b,b} = \{(0, 2\omega b)\}$, the rectilinear orbits in the x_3 axis reduce to the singular origin of $V_{0,b}$ and equatorial (non-circular) ellipses with eccentricity $\tilde{e} = \sqrt{2\sqrt{b^2 - a^2}/(b + \sqrt{b^2 - a^2})}$ project into the singular point $(0, 2\omega b)$ of $V_{a,b}$, $|a| < b$. This corresponds to the physical interpretation of the invariants τ. The energy $\frac{1}{2}\tau_2$ of the equatorial subsystem and the third component $N = (1/2\omega)\tau_4$ of the angular momentum describe the geometry of the projection of the ellipse into the (x_1, x_2) plane. The vertical subsystem has the energy $\frac{1}{2}\tau_3$, and the angle $\arg \tau_1$ determines the synchronisation of (the S^1-families of) the two subsystems.

2.3. Geometrical interpretation

The invariants $(\tau_1, \tau_2, \tau_3, \tau_4)$ and the nodal-Lissajous variables (ℓ, g, ν, L, G, N) are intimately related. Let an axially and oscillatory symmetric Hamiltonian $H \in C^\infty(T^*\mathbb{R}^3)$ be given. By construction the expression in nodal-Lissajous variables does not depend on ν and ℓ. This makes the momenta N and L conjugate to these cyclic angles integrals of motion. Correspondingly, H induces a Hamilton function on $\mathbb{C} \times \mathbb{R}^3$, again denoted by H. The flow of X_H not only keeps the second reduced phase space V invariant, it also has $\{N = a\} \cap \{L = b\}$ as invariant submanifolds. Both argumentations show that the values a and b of N and L act as distinguished parameters of the system.

If $|N| = G$ or $G = L$ the angles ν and ℓ, respectively, of the nodal-Lissajous variables are not well defined. Correspondingly, the ramified 2-torus bundle

$$\tau \circ \sigma : T^*\mathbb{R}^3 \to \mathbb{C} \times \mathbb{R}^3$$

does not have a global section. In fact, the singular fibres are contained in $\{(x, p) \in T^*\mathbb{R}^3 | |N| = G\}$. The defining equation reads $\mathrm{Re}\,\tau_1 = \tau_2(2\omega b - \tau_2)$, and for $a \neq 0$ the sole solution is the singular point $\tau = (0, 2\omega b)$ of $V_{a,b}$. In $V_{0,b}$ the equation may be written as $\tau_1 = |\tau_1|$, yielding the whole upper arc in the plane $\mathrm{Im}\,\tau_1 = 0$ which connects the two singularities $(0, 0)$ and $(0, 2\omega b)$ of the "lemon" $V_{0,b}$. Here $G = 0$, hence these points correspond to (S^1-families of) rectilinear ellipses.

Furthermore, the excluded subset $\{(x, p) \in T^*\mathbb{R}^3 | |N| < G = L\}$ gets reduced to the regular points $\tau = (-(\omega^2/b^2)(b^2 - a^2)^2, (\omega/b)(a^2 + b^2))$ on the lower arc in the intersection of the plane $\operatorname{Im}\tau_1 = 0$ with the twice reduced phase space $V_{a,b}$. These points represent the (S^1-families of) circular ellipses in a plane with inclination $\cos I = a/b$. However, the image of $\{(x, p) \in T^*\mathbb{R}^3 | |N| < G\}$ under $\tau \circ \sigma$ is contractible, making it topologically necessary to exclude one further point in every reduced phase space $V_{a,b}$ to obtain action–angle variables, i.e. a chart onto $\mathbb{T}^3 \times U$, $U \subseteq \mathbb{R}^3$ open.

From Eqs. (2)–(6) the expression of the invariants τ_1, τ_2, τ_3, τ_4 as functions of the nodal-Lissajous variables is easily computed to be

$$\begin{aligned}
\operatorname{Re}\tau_1 &= 2\omega^2\left(1 - \frac{N^2}{G^2}\right)(L^2 - G^2 + L\sqrt{L^2 - G^2}\cos 2g) \\
&\quad -\omega^2\left(1 - \frac{N^2}{G^2}\right)^2 (L + \sqrt{L^2 - G^2}\cos 2g)^2, \\
\operatorname{Im}\tau_1 &= 2\omega^2\left(1 - \frac{N^2}{G^2}\right) G\sqrt{L^2 - G^2}\sin 2g, \\
\tau_2 &= \omega(L - \sqrt{L^2 - G^2}\cos 2g) + \omega\frac{N^2}{G^2}(L + \sqrt{L^2 - G^2}\cos 2g), \\
\tau_3 &= \omega\left(1 - \frac{N^2}{G^2}\right)(L + \sqrt{L^2 - G^2}\cos 2g), \\
\tau_4 &= 2\omega N. \qquad (8)
\end{aligned}$$

Evidently, the angles ν and ℓ do not enter, and Eqs. (8) can be solved to get

$$\begin{aligned}
\cos 2g &= \frac{(\tau_3 - \tau_2)(\tau_2\tau_3 - \operatorname{Re}\tau_1) + \tau_3\tau_4^2}{(\tau_2\tau_3 - \operatorname{Re}\tau_1)\sqrt{2\operatorname{Re}\tau_1 + \tau_2^2 + \tau_3^2 - \tau_4^2}}, \\
\sin 2g &= \frac{\operatorname{Im}\tau_1\sqrt{\tau_4^2 + 2\tau_2\tau_3 - 2\operatorname{Re}\tau_1}}{(\tau_2\tau_3 - \operatorname{Re}\tau_1)\sqrt{2\operatorname{Re}\tau_1 + \tau_2^2 + \tau_3^2 - \tau_4^2}}, \\
L &= \frac{1}{2\omega}(\tau_2 + \tau_3), \qquad G = \frac{1}{2\omega}\sqrt{\tau_4^2 + 2\tau_2\tau_3 - 2\operatorname{Re}\tau_1}, \qquad N = \frac{1}{2\omega}\tau_4. \qquad (9)
\end{aligned}$$

These equations are valid where the nodal-Lissajous variables are defined. The invariants are constrained by the relations $R(\tau) = 0$, $\tau_3 \geq 0$, in particular one may replace $\operatorname{Re}\tau_1$ in (9) by $\tau_3\sqrt{\tau_2^2 - \tau_4^2}\cos(\arg\tau_1)$ and $\operatorname{Im}\tau_1$ by $\tau_3\sqrt{\tau_2^2 - \tau_4^2}\sin(\arg\tau_1)$.

Recall that the angle g gives the position of the semi-minor axis of the ellipse in configuration space, reckoning from the nodal line. In particular g and $g + \pi$ determine the same ellipse when L, G and N are kept fixed. The reduction process is reflected by ℓ measuring the points on the ellipse and ν making up for the whole S^1-family of ellipses. Eqs. (8) and (9) show that the mapping

$$\begin{aligned}
S^1 \times \{(L, G, N) \in \mathbb{R}^3 | |N| < G < L\} &\to V, \\
(g, L, G, N) &\mapsto (\tau_1, \tau_2, \tau_3, \tau_4)
\end{aligned}$$

is a chart that doubly covers the open and dense subset $\{\tau \in \mathbb{C} \times \mathbb{R}^3 | R(\tau) = 0, \tau_3 \geq 0, |N| < G < L\}$ of V.

Fixing the values a of N and b of L we are led to (doubly covering) symplectic co-ordinates (g, G) of the twice reduced phase space $V_{a,b}$. Eqs. (8) and (9) become

$$\begin{aligned}
\operatorname{Re}\tau_1 &= 2\omega^2\left(1-\frac{a^2}{G^2}\right)(b^2-G^2+b\sqrt{b^2-G^2}\cos 2g)\\
&\quad -\omega^2\left(1-\frac{a^2}{G^2}\right)^2(b+\sqrt{b^2-G^2}\cos 2g)^2,\\
\operatorname{Im}\tau_1 &= 2\omega^2\left(1-\frac{a^2}{G^2}\right)\sqrt{b^2-G^2}G\sin 2g,\\
\tau_2 &= \omega(b-\sqrt{b^2-G^2}\cos 2g)+\omega\frac{a^2}{G^2}(b+\sqrt{b^2-G^2}\cos 2g)
\end{aligned}$$

and

$$\begin{aligned}
\cos 2g &= \frac{2\omega b-2\tau_2}{Q}+\frac{4\omega^2a^2(2\omega b-\tau_2)}{(\tau_2(2\omega b-\tau_2)-\operatorname{Re}\tau_1)Q},\\
\sin 2g &= \frac{\operatorname{Im}\tau_1\sqrt{4\omega^2a^2+2\tau_2(2\omega b-\tau_2)-2\operatorname{Re}\tau_1}}{(\tau_2(2\omega b-\tau_2)-\operatorname{Re}\tau_1)Q},\\
G &= \frac{1}{2\omega}\sqrt{4\omega^2a^2+2\tau_2(2\omega b-\tau_2)-2\operatorname{Re}\tau_1},
\end{aligned}$$

where Q is an abbreviation for

$$\sqrt{2\operatorname{Re}\tau_1+\tau_2^2+(2\omega b-\tau_2)^2-4\omega^2a^2}=2\omega\sqrt{L^2-G^2}.$$

To obtain univalued co-ordinates, one may change to $\gamma = 2g$ (and $\Gamma = \frac{1}{2}G$ to make sure that $\mathrm{d}\gamma \wedge \mathrm{d}\Gamma = \mathrm{d}g \wedge \mathrm{d}G$ remains the symplectic structure of the regular part of $V_{a,b}$). This also allows to interpret γ and Γ as polar co-ordinates near $\Gamma = \frac{1}{2}b$ where γ is not defined. The lower boundary $\Gamma = \frac{1}{2}|a|$ corresponds to the singularity of $V_{a,b}$, and for $a = 0$ the whole arc $\tau_1 = |\tau_1|$ is outside the domain of the chart (γ, Γ). On the other hand, the co-ordinates (g, G) may be thought of as a blow-up of the singularity at $\tau = (0, 2\omega b)$ if $a \neq 0$ (and $|a| < b$).

The second reduced phase space V is sliced into the subvarieties $N^{-1}(a) \cap L^{-1}(b) \cong V_{a,b}$. These are surfaces of revolution that extend between $2\omega|a|$ and $2\omega b$, shrinking to a (singular) point for $|a| = b$. Correspondingly, the co-ordinates (γ, Γ) take values in $S^1 \times]\frac{1}{2}|a|, \frac{1}{2}b[$. Fig. 1 shows how the disjoint union $\bigcup V_{a,b}$ fits together to form V, and how (γ, Γ), or (g, G), co-ordinise the different $V_{a,b}$. For a detailed study of the various singularities of V the reader is referred to [12].

To further illustrate the relation between the invariants $\tau_1, \tau_2, \tau_3, \tau_4$ and the nodal-Lissajous variables we have a closer look at the equation

$$|\tau_1|\sin(\arg\tau_1) = 4\omega^2\left(1-\frac{a^2}{4\Gamma^2}\right)\sqrt{b^2-4\Gamma^2}\Gamma\sin\gamma. \tag{10}$$

In [20] the co-ordinates (γ, Γ) are used as cylindrical co-ordinates on a smooth sphere S^2. This yields for $a \neq 0$ a homeomorphism $V_{a,b} \to S^2$ that is a diffeomorphism if the singular point of the turnip and the south pole of the sphere are excluded. From (10) we conclude that the topological circle $\{\arg \tau_1 = 0, \pi\}$ gets mapped to the great circle $\{\gamma = 0, \pi\}$. As $a \to 0$ this topological circle gets more and more distorted within its image great circle. In the limit $a = 0$ the mapping $V_{0,b} \to S^2$ is not longer bijective since the whole arc $\{\arg \tau_1 = 0\}$ gets reduced to the south pole.

In particular, the "left-most points" $(\tau_1, \tau_2, \tau_3, \tau_4) = (0, 2\omega|a|, 2\omega(b - |a|), 2\omega|a|)$ of the turnips have co-ordinates $\Gamma = \frac{1}{2}\sqrt{2|a|(b - |a|)}$, $\gamma = 0$. These points correspond to (S^1-families of) ellipses that project into equatorial circular orbits. For $a = 0$ this is a single rectilinear ellipse in the x_3 axis (for every b) which accounts for the singularity at $(\tau_1, \tau_2, \tau_3, \tau_4) = (0, 0, 2\omega b, 0)$.

3. Normalisation of the Hamilton function

We are given an axially symmetric perturbation H_ε of the isotropic harmonic oscillator H_0 by a cubic potential. In the previous section we have seen how H_ε reduces to a two-degrees-of-freedom system, and how a system that furthermore has the oscillator symmetry may be reduced to one degree of freedom. In this section we normalise H_ε to obtain this oscillator symmetry. The normalisation will be carried out by means of Lie transformations. The process of the normalisation is independent of the set of variables one chooses. We both use the (generalised) action–angle variables and take directly advantage of the flow being periodic, outstanding the advantages and disadvantages of both approaches.

3.1. Lie transformations

In general Lie transformations are used to deal with time-dependently perturbed differential systems, cf. [13,26]. However in this paper, as we treat autonomous Hamiltonian systems, we describe these transformations in this context.

A Lie transformation is a near-identity contact transformation

$$\begin{array}{rccc} \varphi: & T^*\mathbb{R}^3 \times \mathbb{R}^+ & \to & T^*\mathbb{R}^3, \\ & (x', p'; \varepsilon) & \mapsto & (x, p) \end{array}$$

such that $x(x', p'; \varepsilon)$ and $p(x', p'; \varepsilon)$ are the solution of the initial value problem defined by

$$\frac{\mathrm{d}x}{\mathrm{d}\varepsilon} = \frac{\partial W_\varepsilon}{\partial p}, \qquad \frac{\mathrm{d}p}{\mathrm{d}\varepsilon} = -\frac{\partial W_\varepsilon}{\partial x},$$

and initial conditions $x(x', p'; 0) = x'$ and $p(x', p'; 0) = p'$. Thus, the transformation is the time-ε-flow of the Hamilton function W_ε, and as such preserves the Poisson bracket structure.

Deprit [13] introduced the formalism of Lie transformations in the context of a general perturbation theory to deal with perturbed Hamiltonian systems. Therefore the perturbation

technique by using a Lie transformation is usually known as the Lie–Deprit method. We outline the procedure below.

Let H_ε represent a Hamilton function which is developed in power series of the small parameter ε as

$$H_\varepsilon(x, p) = \sum_{n\geq 0} \frac{\varepsilon^n}{n!} H_n^0(x, p). \tag{11}$$

The Lie transformation φ_ε allows to express H_ε in the new variables x' and p', by making use of the Hamilton function

$$W_\varepsilon(x, p) = \sum_{n\geq 0} \frac{\varepsilon^n}{n!} W_{n+1}(x, p).$$

Note that $W_\varepsilon(x, p)$ is conserved under the transformation and thus, it is also expressed as $W_\varepsilon(x', p')$ with the same formal terms W_n. For convenience one continues the coefficient functions of (11) to H_i^j, satisfying the following relation:

$$H_i^j = H_{i+1}^{j-1} + \sum_{0\leq k\leq i} \binom{i}{k} \{H_k^{j-1}, W_{i+1-k}\} \tag{12}$$

for $i \geq 0$ and $j \geq 1$, see Fig. 2. Here $\{\,,\,\}$ denotes the Poisson bracket.

The transformed Hamilton function is denoted by $\bar{H}_\varepsilon$ and reads

$$\bar{H}_\varepsilon(x', p') = \sum_{n\geq 0} \frac{\varepsilon^n}{n!} H_0^n(x', p').$$

The recursion process is sketched by the so-called Lie triangle, see Fig. 2. In each order n of the process the diagonal H_i^j with $i + j = n$ is built starting with H_{n-1}^1 and finishing with H_1^{n-1}. Note that H_0^n cannot be determined due to the fact that W_n is still unknown. Hence, if $\mathcal{L}_{H_0} : F \to \{F, H_0\}$ denotes the Lie operator acting on functions F, then Eq. (12) yields the partial differential equation

$$\mathcal{L}_{H_0}(W_n) + H_0^n = \tilde{H}_0^n, \tag{13}$$

where $\tilde{H}_0^n$ collects all the terms known from the previous order. In this identity, called the *homological equation*, W_n and H_0^n must be determined according to the requirements

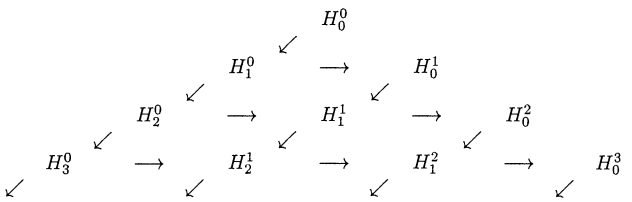

Fig. 2. The Lie triangle.

(averaging over the time, simplification of some type of terms, etc.) of the Lie transformation one performs.

3.2. The normalisation procedure

We consider a Hamilton function $H_\varepsilon(x, p)$ which admits an expansion in powers of the small parameter ε as in (11). In the following we state the concept of the normalisation.

A Lie transformation

$$\varphi : (x', p'; \varepsilon) \mapsto (x, p)$$

is said to normalise the Hamilton function $H_\varepsilon(x, p)$ if the transformed Hamilton function

$$\bar{H}_\varepsilon(x', p') = H_\varepsilon(x(x', p'; \varepsilon), p(x', p'; \varepsilon))$$

is normal (with respect to H_0), that is, it verifies $\{\bar{H}_\varepsilon, H_0\} = 0$, i.e. $\bar{H}_\varepsilon$ is in the kernel of $\mathcal{L}_{H_0}$. Then $\bar{H}_\varepsilon$ is called the normal form series of H_ε.

Now we have to take into account the semi-simple character of H_0. In other words, the matrix corresponding to the linear differential equation associated to H_0 is semi-simple. In this situation, see for instance [44], the algebra $\mathcal{F}$ of functions containing the terms H_n^0 is a direct sum of two subspaces

$$\mathcal{F} = \ker(\mathcal{L}_{H_0}|\mathcal{F}) \oplus \mathrm{im}(\mathcal{L}_{H_0}|\mathcal{F}), \tag{14}$$

where the kernel $\ker(\mathcal{L}_{H_0})$ is the set of functions F such that $\mathcal{L}_{H_0}(F) = 0$ and the image $\mathrm{im}(\mathcal{L}_{H_0})$ is the set of functions ϕ such that there exist functions ψ satisfying $\mathcal{L}_{H_0}(\psi) = \phi$. Normalising H_ε means finding a Lie transformation that projects H_ε onto an element $\bar{H}_\varepsilon$ in $\ker(\mathcal{L}_{H_0}|\mathcal{F})$. It is a geometrical operation, the purpose of which is pushing a symmetry of the Hamilton function of zeroth order through the whole Taylor series of the perturbation. Thus, the normalisation (with respect to the isotropic harmonic oscillator H_0) will allow us to apply the reduction techniques of Section 2.

In practice, the normalisation consists in calculating in each order of perturbation the terms H_0^n of the normal form series together with their corresponding terms W_n in the generating functions, following the algorithm of the Lie transformation. As a rule, the series W_ε and $\bar{H}_\varepsilon$ are divergent. Truncating W_ε at order n, one can transform the Hamilton function H_ε into

$$H_\varepsilon \circ \varphi_\varepsilon = \sum_{k=0}^{n} \frac{\varepsilon^k}{k!} H_0^k(x', p') + \text{higher order terms.}$$

Truncating this expression at order n yields the normal form of order n. Concerning the family (1), we will exclusively work with the normal form $\bar{H}_\varepsilon$ of order 2.

3.3. Normalisation in nodal-Lissajous variables (ℓ, g, ν, L, G, N)

In nodal-Lissajous variables, the process of the normalisation in three degrees of freedom is completely analogous to the one described by Deprit and Elipe [16] in two degrees of

freedom. Introducing one additional degree of freedom, using nodal-Lissajous variables, adds no further complication, because the additional variables (ν, N) are also in the kernel of the Lie derivative, $\mathcal{L}_{H_0}(F) = \{F, H_0\} = \omega(\partial F/\partial \ell)$.

By means of a Lie transformation, when we implement a Lissajous normalisation $\Psi : (\ell', g', \nu', L', G', N') \mapsto (\ell, g, \nu, L, G, N)$, we have to deal with the homological equation (13). Thus, taking

$$H_0^n = (2\pi)^{-1} \int_0^{2\pi} \tilde{H}_0^n \, \mathrm{d}\ell$$

together with

$$W_n = \omega^{-1} \int (\tilde{H}_0^n - H_0^n) \, \mathrm{d}\ell,$$

the normalisation is carried out straightforwardly.

Normalising in nodal-Lissajous variables means "removing the dependence on the variable ℓ" up to a certain order, obtaining an averaged orbit with respect to the elliptic anomaly. The feature of the nodal-Lissajous variables when normalising is precisely that the physical meaning of this process is well reflected, whereas in other variables it is not. The results obtained have been widely checked with `Mathematica`. Truncating after second-order terms, the normal form of H_ε yields

$$\bar{H}_\varepsilon = \omega L + \frac{\varepsilon^2 L^2}{96\omega^4}(C_0 + C_2 \cos 2g + C_4 \cos 4g), \tag{15}$$

where

$$C_0 = 8\beta^2(-6+e^2)+8\beta(2(\beta-3\alpha) + e^2(\alpha - 7\beta))s^2 + 5(\alpha+\beta)(3\beta-\alpha)(2+e^2)s^4,$$
$$C_2 = 20(\alpha+\beta)es^2(-2\beta + (3\beta-\alpha)s^2), \qquad C_4 = 5(\alpha+\beta)(3\beta-\alpha)e^2 s^4.$$

Primes have been dropped in order to simplify the notation. Recall that the state functions e and s are given by $e^2 = 1 - (G^2/L^2)$ and $s^2 = 1 - (N^2/G^2)$.

3.4. *Normalisation in complex variables* (z_1, z_2, z_3)

What we do here is to apply the algorithm of the normalisation in complex variables (4). It turns out to be advantageous to complete the $z_j = \omega x_j + \mathrm{i} p_j$ by their complex conjugate $u_j = \omega x_j - \mathrm{i} p_j$, thereby defining a transformation of co-ordinates and momenta between the sets $T^*\mathbb{R}^3$ and $CS = \{(z, u) \in T^*\mathbb{C}^3 | u = \bar{z}\}$, as

$$\begin{array}{rccc} \Upsilon: & T^*\mathbb{R}^3 & \to & CS, \\ & (x, p) & \mapsto & (z, u) \end{array}$$

which is not singular anywhere in $T^*\mathbb{R}^3$; its inverse is the transformation given by the equations

$$x = \frac{z+u}{2\omega}, \qquad p = \frac{z-u}{2\mathrm{i}}.$$

The transformation Υ induces the Poisson bracket $\{z_k, u_j\} = -2\omega \mathrm{i}\delta_{kj}$, which is non-standard. More importantly, the Lie derivative $\mathcal{L}_{H_0}$ of a function F associated to H_0, defined through the Poisson bracket $\{F, H_0\}$, becomes the diagonal differential operator

$$\mathcal{L}_{H_0} = -\omega \mathrm{i}\left(z_1\frac{\partial}{\partial z_1} - u_1\frac{\partial}{\partial u_1} + z_2\frac{\partial}{\partial z_2} - u_2\frac{\partial}{\partial u_2} + z_3\frac{\partial}{\partial z_3} - u_3\frac{\partial}{\partial u_3}\right),$$

because the unperturbed Hamilton function in the complex variables reads

$$H_0 = \tfrac{1}{2}(z_1u_1 + z_2u_2 + z_3u_3).$$

Yet, as the perturbation remains polynomial in the complex variables, for a given monomial $m = z_1^j z_2^k z_3^l u_1^r u_2^s u_3^t$ (j, k, l, r, s and t being non-negative integers) its Lie derivative yields $\mathcal{L}_{H_0}(m) = -\omega \mathrm{i}(j+k+l-r-s-t)m$. The kernel of $\mathcal{L}_{H_0}$ is the vector subspace generated by the monomials m such that their corresponding exponents verify the relation

$$j + k + l - r - s - t = 0. \tag{16}$$

Hence, the normalisation for a potential written in the (z, u) is as follows. On the one hand a term m of the perturbing potential which satisfies (16) does not contribute to the generator and remains in the normalised potential. On the other hand if m does not verify (16) its contribution to the normalised Hamiltonian is zero and the term

$$\frac{\mathrm{i}m}{\omega(j + k + l - r - s - t)}$$

is added to the generator W_ε. The application of the normalisation in complex variables up to order $2n$ yields that

$$H_\varepsilon \circ \varphi_\varepsilon = \sum_{i=0}^{n} \frac{\varepsilon^{2i}}{(2i)!} H_0^{2i} + \mathcal{O}(\varepsilon^{2n+2}),$$

where $H_0^0 = H_0$ is the Hamilton function of the isotropic harmonic oscillator. Each coefficient function H_0^{2i}, $i = 1, 2, \ldots, n$, is a homogeneous polynomial in the complex variables (z, u) (as well as in the real variables (x, p)) of degree $2i + 2$ and all the terms verify (16). Note that odd coefficient functions are zero because $\{H_0^i, H_0\} = 0$ implies that i is even. Up to second order the normal form of H_ε reads

$$\begin{aligned}\bar{H}_\varepsilon = \frac{1}{2}(z_1u_1 + z_2u_2 + z_3u_3) - \frac{\varepsilon^2}{48\omega^6}(&5\alpha^2 z_3^2u_3^2 + \alpha\beta(12(z_1u_1 + z_2u_2)z_3u_3 \\ &- z_3^2(u_1^2 + u_2^2) - (z_1^2 + z_2^2)u_3^2) + \beta^2(6z_3^2(u_1^2 + u_2^2) + 5z_1^2u_1^2 + 5z_2^2u_2^2 \\ &+ 8(z_1u_1 + z_2u_2)z_3u_3 + 6(z_1^2 + z_2^2)u_3^2 + 12z_1u_1z_2u_2 - z_1^2u_2^2 - z_2^2u_1^2)),\end{aligned} \tag{17}$$

where primes have been dropped. Note that this normal form still has to be expressed in the invariants (6a) and (6b).

As expected the normalisation gives the same results in both sets of variables. However, if one needs to reach a high order normalisation, the complex variables are a better choice. The main reason is that an algebraic manipulator of general purpose (`Mathematica`, `Maple`,

etc.) handles polynomials faster than expressions involving at the same time polynomials and trigonometric terms, as it happens with the nodal-Lissajous variables. It turns out that the performance of the complex variables z_j can still be improved upon by working with the complex invariants σ_j.

3.5. *Normalisation in invariants* $(\sigma_1, \sigma_2, \sigma_3)$

Here we proceed along the lines of the previous subsection and complete the σ_j of (3) by $\sigma_4 := \bar{\sigma}_1$, $\sigma_5 := \bar{\sigma}_2$ and $\sigma_6 := \bar{\sigma}_3$. Hence,

$$H_0(\sigma) = \tfrac{1}{4}(\sigma_2 + \sigma_5) + \tfrac{1}{2}\sigma_3\sigma_6,$$

and the Poisson structure becomes the one depicted in Table 1, cf. [12].

The important point is again that the Lie operator $\mathcal{L}_{H_0}$ is diagonal, indeed

$$\mathcal{L}_{H_0} = -\omega \mathrm{i}\left(2\sigma_1\frac{\partial}{\partial\sigma_1} + \sigma_3\frac{\partial}{\partial\sigma_3} - 2\sigma_4\frac{\partial}{\partial\sigma_4} - \sigma_6\frac{\partial}{\partial\sigma_6}\right)$$

and thus maps a monomial $m = \sigma_1^j\sigma_2^k\sigma_3^l\sigma_4^r\sigma_5^s\sigma_6^t$ to $\mathcal{L}_{H_0}(m) = -\omega\mathrm{i}(2j + l - 2r - t)\, m$. Recall from (3) that $\sigma_1, \sigma_2, \sigma_4$ and σ_5 are of degree 2 in the z_j, u_j. Correspondingly, we call m of degree $2j + 2k + l + 2r + 2s + t$. The kernel of $\mathcal{L}_{H_0}$ is the vector subspace generated by the monomials m such that their corresponding exponents verify the relation

$$2j + l - 2r - t = 0. \tag{18}$$

Hence, the normalisation for a potential written in the σ_j is as follows. On the one hand a term m of the perturbing potential which satisfies (18) does not contribute to the generator W_ε and remains in the normalised potential. On the other hand if m does not verify (18) its contribution to the normalised Hamiltonian is zero and the term

$$\frac{\mathrm{i}m}{\omega(2j + l - 2r - t)}$$

Table 1
The Poisson brackets of the σ_j's

$\{A, B\}$	σ_1	σ_2	σ_3	σ_4	σ_5	σ_6	B
σ_1	0	$-4\mathrm{i}\omega\sigma_1$	0	$-4\mathrm{i}\omega(\sigma_2+\sigma_5)$	$-4\mathrm{i}\omega\sigma_1$	0	
σ_2	$4\mathrm{i}\omega\sigma_1$	0	0	$-4\mathrm{i}\omega\sigma_4$	0	0	
σ_3	0	0	0	0	0	$-2\mathrm{i}\omega$	
σ_4	$4\mathrm{i}\omega(\sigma_2+\sigma_5)$	$4\mathrm{i}\omega\sigma_4$	0	0	$4\mathrm{i}\omega\sigma_4$	0	
σ_5	$4\mathrm{i}\omega\sigma_1$	0	0	$-4\mathrm{i}\omega\sigma_4$	0	0	
σ_6	0	0	$2\mathrm{i}\omega$	0	0	0	
A							

is added to the generator. The application of the normalisation in the invariants σ_j up to degree $2n$ yields that

$$H_\varepsilon \circ \varphi_\varepsilon = \sum_{i=0}^{n} \frac{\varepsilon^{2i}}{(2i)!} H_0^{2i} + \mathcal{O}(\varepsilon^{2n+2}),$$

where $H_0^0 = H_0$ is the Hamilton function of the isotropic harmonic oscillator. Each coefficient function H_0^{2i}, $i = 1, 2, \ldots, n$, is a polynomial (homogeneous of degree $2i + 2$ if expressed in the variables z_j, u_j). As expected, again odd coefficient functions vanish. The algorithm now yields the normal form already expressed in the invariants, the passage to the σ_j having occurred before the normalisation. Since the normalisation introduces the oscillator symmetry and since the τ_j are delineated to express the normal form of an axially symmetric Hamilton function, we may write the second-order normal form $\bar{H}_\varepsilon$ in the τ_j as

$$\bar{H}_\varepsilon = \frac{1}{2}(\tau_2 + \tau_3) + \frac{\varepsilon^2}{48\omega^6}(\alpha\beta(\tau_1 + \bar{\tau}_1 - 12\tau_2\tau_3) - 5\alpha^2\tau_3^2 - \beta^2(6(\tau_1 + \bar{\tau}_1) + 6\tau_2^2 + 8\tau_2\tau_3 - \tau_5)). \tag{19}$$

Of course, (17) and (15) express this same function in the z_j, u_j variables and the nodal-Lissajous variables, respectively. The important point is always that the Lie operator $\mathcal{L}_{H_0}$ is diagonal and, hence, the splitting (14) is immediate. However, the procedure in the σ_j involves the computation of less partial derivatives than its version in the z_j, u_j. The reason is the form adopted by the Lie operator $\mathcal{L}_{H_0}$ in both sets of variables. Hence, the best option seems to be to perform the normalisation with the invariants σ_j.

4. The one-degree-of-freedom problem

In this section we describe the flow of the averaged system on the twice reduced phase space $V_{a,b}$. In fact the problem defines a one-degree-of-freedom system because we have reduced the normal form of the original system twice, as explained in Section 2. We give the possible phase portraits according to 2 parameters, which are functions of the 4 parameters of the problem, the external parameters α and β and the fixed values a, b of N and L, respectively. There are two possible ways of approaching the study of the dynamics of this problem. One consists in setting up the differential equations corresponding to $\bar{H}_\varepsilon$ and discuss the existence and number of solutions of this system equated to zero. This gives the equilibria after testing that they belong to $V_{a,b}$. We refer the reader to [58] for an exposition along these lines. An alternative approach is the one we follow here and uses geometrical tools in order to calculate the equilibria and their bifurcations.

4.1. Parameter reduction

The Hamilton function (1) and its normal form (19) depend on the external parameters α, β in a redundant way. Rather than putting $\alpha =: \cos\phi$, $\beta =: \sin\phi$ as done in [45], we scale α away and use $\lambda := (\beta/\alpha)$ as sole parameter. In this way we lose the case $\alpha = 0$,

but it turns out that for sufficiently large $|\lambda|$ no further changes occur and "$\lambda = \infty$" can be easily incorporated again. Recall that ε merely expresses the smallness of the perturbing force field (or, equivalently, how close to the origin we consider the dynamics). Our final results in Section 5 will concern $\varepsilon > 0$ sufficiently small.

For fixed values a and b of N and L, respectively, we can eliminate $\tau_3 = 2\omega b - \tau_2$, $\tau_4 = 2\omega a$ and $\tau_5 = \tau_2^2 - 4\omega^2 a^2$. In this way the normal form (19) becomes dependent on the distinguished parameters a and b and induces

$$\bar{H}_\varepsilon^{a,b;\lambda} = \omega b + \frac{\varepsilon^2}{48\omega^6}(-20\omega^2 b^2 - 4\omega^2\lambda^2 a^2 + 2\lambda(1-6\lambda)\mathrm{Re}\,\tau_1 + 4\omega(5-6\lambda-4\lambda^2)b\tau_2 - (5-12\lambda-3\lambda^2)\tau_2^2)$$

on the twice reduced phase space $V_{a,b}$. To further simplify we scale

$$\tau_1 \mapsto 4\omega^2 b^2 \tau_1, \qquad \tau_2 \mapsto 2\omega b \tau_2, \qquad a \mapsto ba, \tag{20}$$

divide $\bar{H}_\varepsilon^{a,b;\lambda}$ by $(\varepsilon^2 b^2/12\omega^4)$, omit constant terms and rescale time. This shows that also the distinguished parameters a, b are redundant and only their ratio $\mu = a/b$ is relevant for the dynamics of the reduced system. The twice reduced phase space becomes in this way

$$V_\mu = \{\tau \in \mathbb{C} \times [|\mu|, 1] | R_\mu(\tau) = 0\}$$

with $R_\mu(\tau) = (\mathrm{Re}\,\tau_1)^2 + (\mathrm{Im}\,\tau_1)^2 - (\tau_2 - 1)^2(\tau_2^2 - \mu^2)$. The Poisson bracket (7) turns into

$$\{f, g\} = (\nabla f \times \nabla g | \nabla R_\mu)$$

and the Hamilton function $\bar{H}_\varepsilon^{a,b;\lambda}$ leads to

$$\mathcal{H}^\lambda(\tau) = 2\lambda(1-6\lambda)\mathrm{Re}\,\tau_1 + 2(5-6\lambda-4\lambda^2)\tau_2 - (5-12\lambda-3\lambda^2)\tau_2^2. \tag{21}$$

Note that the dependence of (21) on the external parameter λ and the dependence of the phase space V_μ on μ makes the Hamiltonian system defined in this way a family that depends on 2 parameters.

For an open and dense part of the parameter plane we expect $\mathcal{H}^\lambda$ to be a *Morse function* on V_μ, i.e. having finitely many saddles and (local) extrema which are all non-degenerate. These lead to saddles and centres of the phase flow, furthermore the singular points of V_μ are always equilibria. To be more explicit, the orbits are the intersections of the level sets $\{\mathcal{H}^\lambda(\tau) = h\}$ with V_μ in $\mathbb{C} \times \mathbb{R}$. From this the phase portraits are easily obtained by geometric considerations.

At parameter values where the Hamilton function fails to be a Morse function, the system is subject to bifurcations. We remark here that the usual definition of a Morse function $\mathcal{F}$ requires $\mathcal{F}$ to assume different values at its saddles and (local) extrema. However, there are no dynamical consequences if the energy assumes the same value on two different centres, or on a centre and a saddle. Therefore, we do not speak of a bifurcation in such cases. On the other hand two saddles may become connected by heteroclinic orbits if they have the same energy. We will see that this does not happen for $\mathcal{H}^\lambda$ on V_μ. The various bifurcation lines (and points) are given in Fig. 3. Most bifurcations involve the equilibria at the singular points; when passing through the curve C a centre–saddle (or Hamiltonian saddle–node)

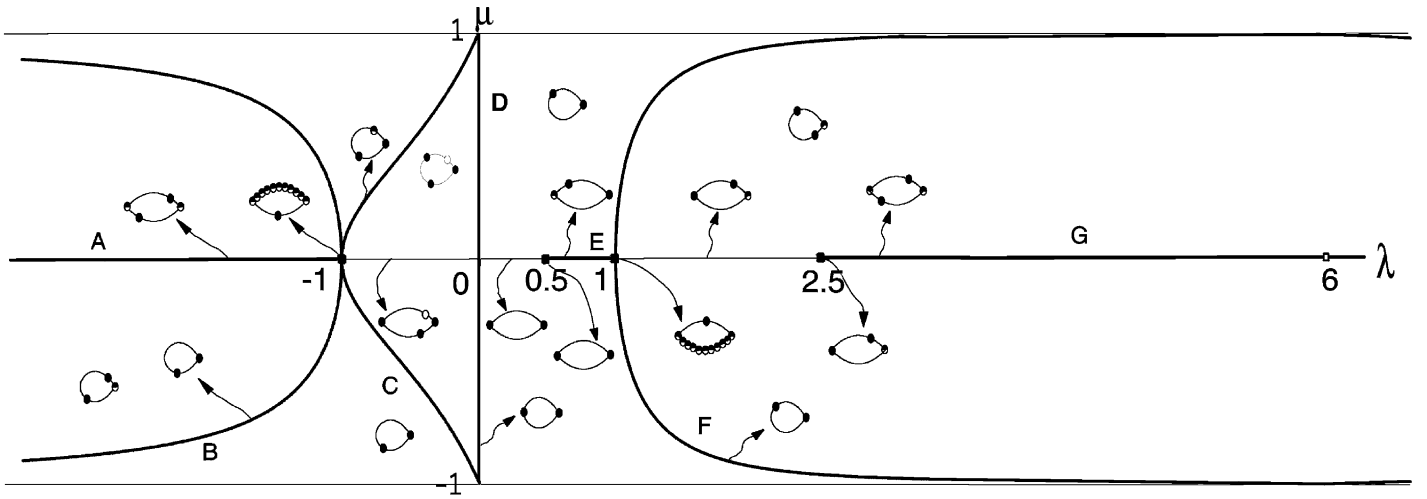

Fig. 3. Bifurcation diagram and meridian sections Im $\tau_1 = 0$ of turnips and lemons. Dynamically stable equilibria have index $+1$ and are characterised by a black circle. Equilibria of index 0 and -1 are dynamically unstable and are depicted by a black–white or white circle, respectively. At $\lambda = 6$ the curve F touches $\mu = \pm 1$. The flow for (λ, μ) in the small wedges between F and $\mu = \pm 1$ when $\lambda > 6$ is equivalent to the one for (λ, μ) in the region bounded by B, C and $\mu = \pm 1$. For $(\lambda, \mu) = (\pm 1, 0)$ a whole arc is filled with equilibria of index 0.

bifurcation occurs. In Fig. 3 we have also assembled sketches of the various phase portraits. Indeed, these are governed by the occurring equilibria, and as we see in Section 4.2 all equilibria occur in the meridian section $\{\mathrm{Im}\,\tau_1 = 0\}$ of V_μ. The fact that V_μ decreases to a point as $|\mu| \to 1$ is not reflected in the illustrations of Fig. 3. We also remark that the bifurcation diagram is symmetric with respect to the λ axis.

We stress that one has to be careful when interpreting the bifurcation diagram. The parameter μ is distinguished with respect to λ in that only reparametrisations of the form

$$(\lambda, \mu) \mapsto (\tilde{\lambda}(\lambda), \tilde{\mu}(\lambda, \mu))$$

are allowed to ensure that the new $\tilde{\mu}$ can still be interpreted as a ratio of values of phase space variables. Recall that μ can simply be altered by a change of initial conditions, while a change of λ corresponds to a different perturbing force field.

This gives the parameter plane a fibred structure; rather than being a plain 2-parameter family depending on (λ, μ), our one-degree-of-freedom systems are 1-parameter families (depending on λ) of 1-parameter families of Hamiltonian systems, the latter depending on the distinguished parameter μ. This affects the interpretation of bifurcations. What we are interested in are those values of λ for which $\mathcal{H}^\lambda$ defines a structurally stable 1-parameter family on V_μ. From Fig. 3 we infer immediately that this does not hold true when λ takes one of the six values in the set $\{-1, 0, \frac{1}{2}, 1, \frac{5}{2}, 6\}$. It turns out that these are the only exceptional values.

Theorem 4.1. *For all values of λ excepting those in the set $\{-1, 0, \frac{1}{2}, 1, \frac{5}{2}, 6\}$ the 1-parameter family of Hamiltonian systems defined by $\mathcal{H}^\lambda$ on V_μ is structurally stable.*

The proof of this theorem is given in Sections 4.2–4.4. We first identify the occurring equilibria. Then we study where these undergo bifurcations. Finally we show that these bifurcations are versally unfolded by means of the distinguished parameter μ (unless λ takes one of the exceptional values).

4.2. Equilibria

The equilibria of the Hamiltonian system defined by $\mathcal{H}^\lambda$ on V_μ are those points where $\nabla\mathcal{H}^\lambda$ is parallel to ∇R_μ. Geometrically, this means that (within $\mathbb{R}^3$) the level set $\{\mathcal{H}^\lambda(\tau) = h\}$ is tangent to the phase space V_μ. This is always the case at the singularities of V_μ. The systems defined by (1) are reversible with respect to $p \mapsto -p$, and this reflection is preserved as $\mathrm{Im}\,\tau_1 \mapsto -\mathrm{Im}\,\tau_1$. Now $\mathcal{H}^\lambda$ is even independent of the variable $\mathrm{Im}\,\tau_1$ whence the level sets and à fortiori their tangent planes contain the $\mathrm{Im}\,\tau_1$ axis. As V_μ is a surface of revolution, a tangent plane to V_μ can only contain the $\mathrm{Im}\,\tau_1$ axis in points where $\mathrm{Im}\,\tau_1$ vanishes. Thus, all equilibria are confined to the meridian section $V_\mu \cap \{\mathrm{Im}\,\tau_1 = 0\}$. This contour in the $(\mathrm{Re}\,\tau_1, \tau_2)$ plane is given by

$$\mathrm{Re}\,\tau_1 = \pm(\tau_2 - 1)\sqrt{\tau_2^2 - \mu^2}, \quad |\mu| \le \tau_2 \le 1 \tag{22}$$

and the intersection $\{\mathcal{H}^\lambda(\tau) = h\} \cap \{\mathrm{Im}\,\tau_1 = 0\}$ is the parabola

$$\mathrm{Re}\,\tau_1 = \frac{1}{2\lambda(1-6\lambda)}((5 - 12\lambda - 3\lambda^2)\tau_2^2 - 2(5 - 6\lambda - 4\lambda^2)\tau_2 + h). \tag{23}$$

It is geometrically clear that for each fixed λ and μ the "height" of this parabola can always be adjusted in such a way that (22) and (23) touch. An explicit formula can be obtained equating the derivatives of the right-hand sides of (22) and (23) with respect to τ_2. Recalling $\operatorname{Im}\tau_1 = 0$, this yields the positions of the equilibria (as depicted in Fig. 3).

Where the nodal-Lissajous variables are defined they provide an alternative way to compute the equilibria. To simplify the equations one uses the state functions e, s and η which allow for expressions without explicit square roots. We refer to [58] for more details.

The cases $\lambda = 0$ and $\lambda = \frac{1}{6}$ immediately appear to be special situations. Here the level sets $\{\mathcal{H}^\lambda(\tau) = h\}$ are planes perpendicular to the τ_2 axis. All orbits are equivariant with respect to rotations about this axis and the sole equilibria occur at $\tau = (0, |\mu|)$ and $\tau = (0, 1)$. These both have index $+1$.

We recall that in both these cases the original system (1) is integrable. But while $\mathcal{H}^{1/6}$ defines a structurally stable family of flows on V_μ, the flows defined by $\mathcal{H}^0$ on V_μ are not structurally stable. The reason is that in this latter case the equilibrium at $\tau = (0, 1)$ is degenerate for all $\mu \in [-1, 1]$.

4.3. Bifurcations

We treat bifurcations of regular equilibria and of the equilibria in the singular points of V_μ as different cases.

4.3.1. The equilibria at $\tau = (0, 1)$

The meridian section (22) defines at the singular point $\tau = (0, 1)$ the cone

$$\operatorname{Re}\tau_1 = \pm\sqrt{1-\mu^2}(\tau_2 - 1), \quad \tau_2 \le 1.$$

Thus there are three possibilities for the parabola (23) to pass through $\tau = (0, 1)$.

The parabola may pass "outside" the cone, which means that the modulus of the slope is larger than $\sqrt{1-\mu^2}$. In this case the equilibrium is dynamically stable and has index $+1$. We say that the system has a centre at this singular point.

When the modulus of the slope is less than $\sqrt{1-\mu^2}$, the parabola passes "inside" the cone and the equilibrium is dynamically unstable. Although it has index 0, we say that a saddle occurs at this singular point. Obviously both cases are structurally stable, i.e. the dynamic properties near $\tau = (0, 1)$ are not altered by sufficiently small changes of the system.

The third possibility is that the parabola passes with slope $\pm\sqrt{1-\mu^2}$ through the singular point. Here a bifurcation occurs, under variation of μ the centre at $\tau = (0, 1)$ turns into a saddle and a centre (at some regular point) splits off, or vice versa. Note that (except for $\lambda = \pm 1$) the bifurcating equilibrium is still dynamically stable with index $+1$. The bifurcation lines concerning the equilibria at $\tau = (0, 1)$ are defined by the equation

$$\lambda^2 - 6\lambda = \pm\sqrt{1-\mu^2}(\lambda - 6\lambda^2),$$

i.e. consist of the μ axis D and the curves B and F in Fig. 3 given by

$$\mu^2 = \frac{35(\lambda^2 - 1)}{(1 - 6\lambda)^2}.$$

In particular, we have $\mu = \pm 1$ for $\lambda = 6$. Here the single point of $V_{\pm 1}$ bifurcates.

4.3.2. The equilibrium at $\tau = (0, 0)$

In this case (22) defines the cone $\mathrm{Re}\,\tau_1 = \pm\tau_2$, $\tau_2 \geq 0$ and we distinguish again three possibilities. However, the singularity at $\tau = (0, 0)$ is not present for $\mu \neq 0$ and these three possibilities entail different implications.

When the parabola passes "outside" the cone, having a slope of modulus larger than 1, the system has a centre at this singular point. This is a structurally stable situation because for sufficiently small $|\mu| \neq 0$ the parabola touches the pertinent meridian contour at some regular point $\hat{\tau}$ close to zero where the system has a centre as well.

When the slope lies in $]-1, 1[$ the singular point is a saddle with index 0. Together with the (un)stable manifold we may think of an "orbit with period ∞". For sufficiently small $|\mu| \neq 0$ there are nearby orbits with very large period, but no equilibria. This yields the bifurcation lines $A = \{(\lambda, 0)|\lambda < -1\}$, $E = \{(\lambda, 0)|\frac{1}{2} < \lambda < 1\}$ and $G = \{(\lambda, 0)|\lambda > \frac{5}{2}\}$ of Fig. 3. We discuss in Section 4.5 below why we expect the system to have *monodromy* for these λ-values.

At the boundary points $\lambda = -1, \frac{1}{2}, 1, \frac{5}{2}$ (but not at "$\lambda = \infty$") the slope of the parabola through $\tau = (0, 0)$ has modulus 1. Obviously these equilibria are not structurally stable. For $\lambda = \frac{1}{2}, \frac{5}{2}$ the bifurcating equilibrium is dynamically stable with index $+1$.

At $\lambda = \pm 1$ the situation is much more degenerate. Still keeping $\mu = 0$, the parabola through $\tau = (0, 0)$ coincides with the whole upper or lower arc of the meridian section, respectively, yielding continua of degenerate equilibria. Recall that for $\lambda = 1$ the original system (1) is integrable and that $\lambda = -1$ is the 3D Hénon–Heiles case, cf. [21,22,58]. We discuss the behaviour at the boundary points $\lambda = -1, \frac{1}{2}, 1, \frac{5}{2}$ to some more extent in Section 4.5.

4.3.3. The equilibria at regular points

Where regular equilibria bifurcate the parabola (23) touches the meridian section (22) in a degenerate way. As shown in [12], such a bifurcation must be a centre–saddle bifurcation. Also, for fixed λ there can never be more than one centre–saddle bifurcation under variation of $\mu \geq 0$. For such a bifurcation to occur it is necessary (though not sufficient) that the extremum of the parabola (23) is taken at some $\hat{\tau}_2$ between 0 and 1. In case this extremum is a maximum, the bifurcation occurs on the upper arc of the meridian section. If it is a minimum, the bifurcation occurs on the lower arc.

When $|\mu|$ varies through $[0, 1]$, the lemon becomes a turnip which shrinks to a point as $|\mu| \to 1$, but always contains the singular point $\tau = (0, 1)$. This shows that the extremum of the parabola (23) has in fact to be taken at some $\hat{\tau}_2 \in [\frac{1}{2}, 1]$. This happens for $\lambda \in [-1, 0] \cup [1, 6]$, see Fig. 4. The modulus of the curvature of the meridian section (22) equals 1 for $\mu = 0$ and increases in all points $\tau_2 \in [|\mu|, 1]$ as $|\mu|$ approaches 1. For a centre–saddle bifurcation to occur the curvature $\kappa = \frac{1}{2}p''_\lambda$ (denoting by "$'$" the derivative with respect to τ_2) of the right-hand side p_λ of (23) has therefore to be ≤ -1 for $\lambda \in [-1, 0]$

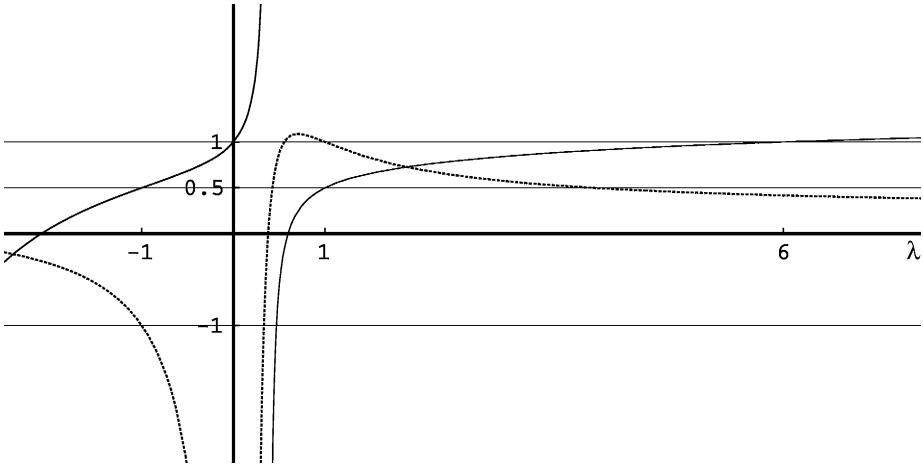

Fig. 4. The dotted function is the curvature κ of the right-hand side p_λ of (23). The other function gives the position $\hat{\tau}_2$ of the extremum of the parabola $p_\lambda(\tau_2)$.

and ≥ 1 for $\lambda \in [1, 6]$. This proves that there are no centre–saddle bifurcations for $\lambda \in [1, 6]$ and that there is for each $\lambda \in [-1, 0]$ exactly one $\hat{\mu} > 0$ such that $\mathcal{H}^\lambda$ undergoes on V_μ a centre–saddle bifurcation as μ passes through $\hat{\mu}$ or through $-\hat{\mu}$, see again Fig. 4.

To obtain an analytic expression for the curve C in Fig. 3 we consider, next to p_λ, the right-hand side q_μ of (22). We are looking for points $\tau_2 \in [|\mu|, 1]$ where the 2-jets of both functions are equal. Since we can always choose h to make $p_\lambda(\tau_2) = q_\mu(\tau_2)$ in some prescribed point τ_2, we only have to equate the first and second derivatives. It is more efficient to work with polynomials, so we define

$$f(\tau_2) := (\tau_2^2 - \mu^2)((p'_\lambda(\tau_2))^2 - (q'_\mu(\tau_2))^2)$$

and search for points $\tau_2 \in [|\mu|, 1]$ where both f and its derivative vanish. In fact, we are not interested in the points τ_2 themselves, but in the induced relation between λ and μ. The proper tool to achieve this goal is the discriminant of f, i.e. the resultant of the two polynomials f and f', see [9] for the definition and the properties of the resultant. The relevant factor turns out to be

$$\begin{aligned}
&5(\lambda+1)(\lambda-1)(2\lambda-1)^3(2\lambda-5)^3 + 3(18576\lambda^8 - 23136\lambda^7 - 11992\lambda^6 \\
&\quad +21048\lambda^5 + 14709\lambda^4 - 34680\lambda^3 + 21750\lambda^2 - 6000\lambda + 625)\mu^2 \\
&\quad +15(\lambda+1)(\lambda-1)(2\lambda-1)(2\lambda-5)(3\lambda-1)^2(9\lambda-5)^2\mu^4 \\
&\quad -5(\lambda+1)(\lambda-1)(3\lambda-1)^3(9\lambda-5)^3\mu^6
\end{aligned}$$

and is of degree 3 in μ^2. Hence, it can be solved, yielding μ^2 as a function of λ on the interval $[-1, 0]$, i.e. the curve C of Fig. 3.

The centre–saddle bifurcations all take place within the charts (γ, Γ) provided by the nodal-Lissajous variables. Thus, an alternative way to compute the curve C is to look for

degenerate equilibria in these variables. To simplify the expressions one uses the state functions e, s and η which allow to write the equations of motion without explicit square roots. In this way Yanguas [58] obtains polynomials $\mathcal{P}_4^1$ and $\mathcal{P}_4^2$ of degree 4, the roots of which yield the equilibria on the upper and lower arc of (22), respectively. We remark that this approach leads to simpler formulae. For instance, compared with the discriminant of $\mathcal{P}_4^1$ the discriminant of f has an "extra factor".

Remark. For parameter values off the curve C all regular equilibria are non-degenerate. For a centre the parabola (23) has to lie "outside" of the contour (22), and vice versa in the neighbourhood of a saddle. Alternatively, one could compute the eigenvalues of the linearisation of the equations of motion

$$\frac{\mathrm{d}}{\mathrm{d}t}\mathrm{Re}\,\tau_1 = \{\mathrm{Re}\,\tau_1, \mathcal{H}^\lambda\}, \qquad \frac{\mathrm{d}}{\mathrm{d}t}\mathrm{Im}\,\tau_1 = \{\mathrm{Im}\,\tau_1, \mathcal{H}^\lambda\}, \qquad \frac{\mathrm{d}}{\mathrm{d}t}\tau_2 = \{\tau_2, \mathcal{H}^\lambda\}.$$

Note that the constraint $R_\mu(\tau) = 0$ forces one of these eigenvalues to vanish. The other two eigenvalues characterise the linearised flow on V_μ.

4.3.4. Global bifurcations

To prove that there are no global bifurcations we show that whenever there are two (or more) saddles, these do not have the same energy. Now there is at most one saddle on V_μ except when $\mu = 0$ and $\lambda \in]-\infty, -1[\cup]\frac{5}{2}, \infty[$ where both singular points are saddles. On the other hand

$$\mathcal{H}^\lambda(0,0) = \mathcal{H}^\lambda(0,1) \Leftrightarrow \lambda = \pm 1.$$

We have already remarked that the flows defined by $\mathcal{H}^{\pm 1}$ on V_0 are very degenerate.

4.4. Structurally stable families

To conclude the proof of Theorem 4.1 we have to show that the bifurcations of the previous section are, for fixed $\lambda \notin \{-1, 0, \frac{1}{2}, 1, \frac{5}{2}, 6\}$, versally unfolded under variation of μ. For the centre–saddle bifurcation this has been shown in [12]. Furthermore, it is obvious that sufficiently small perturbations do not alter the qualitative behaviour of the one-degree-of-freedom family as (λ, μ) passes through $A \cup E \cup G$. Since there are no global bifurcations, only the passage through $B \cup F$ remains to be understood.

The equilibria at $\tau = (0, 1)$ stand for (S^1-families of) equatorial ellipses. These are invariant under a π-rotation about the vertical axis and it is exactly this non-trivial isotropy which is responsible for the singularity. To resolve it, one has to pass to a 2:1 covering, e.g. given by

$$\mathrm{Re}\,\tau_1 = \tfrac{1}{4}(u^2 - v^2), \qquad \mathrm{Im}\,\tau_1 = \tfrac{1}{2}uv, \qquad \tau_2 = \tfrac{1}{2}(w + 1) \tag{24}$$

with the relation $R_\mu(\tau) = 0$ becoming

$$16R_\mu(u, v, w) = (u^2 + v^2)^2 - (w - 1)^2((w + 1)^2 - 4\mu^2) = 0. \tag{25}$$

To obtain the correct time scale we replace (25) by the equivalent relation

$$Q_\mu(u, v, w) = \tfrac{1}{2}(u^2 + v^2) + \tfrac{1}{2}(w - 1)\sqrt{(w + 1)^2 - 4\mu^2} = 0. \tag{26}$$

When $\mu = 0$ this relation defines the sphere $u^2 + v^2 + w^2 = 1$ and $u, v, -w$ are the well-known Hopf variables describing the 1–1 resonance, cf. [10,11,15]. On $U_\mu := \{(u, v, w) \in \mathbb{R}^3 | Q_\mu(u, v, w) = 0, 2|\mu| - 1 \leq w \leq 1\}$ the Hamilton function turns into

$$\mathcal{H}^\lambda(u, v, w) = \tfrac{1}{2}\lambda(1 - 6\lambda)(u^2 - v^2) + \tfrac{5}{2}(1 - \lambda^2)w - \tfrac{1}{4}(5 - 12\lambda - 3\lambda^2)w^2,$$

where we omit constant terms. The Poisson bracket is given by the vector triple product $\{f, g\} = (\nabla f \times \nabla g | \nabla Q_\mu)$. By construction the system is equivariant with respect to the π-rotation

$$(u, v, w) \mapsto (-u, -v, w),$$

i.e. the system on the 2:1 covering is $\mathbb{Z}_2$-symmetric. Passing back to the co-ordinates $(\mathrm{Re}\,\tau_1, \mathrm{Im}\,\tau_1, \tau_2)$ would exactly mean to reduce this $\mathbb{Z}_2$-symmetry. We remark that for $\mu \neq 0$ the nodal-Lissajous variables (g, G) provide co-ordinates on the 2:1 covering U_μ near the desingularised point $(u, v, w) = (0, 0, 1)$ that behave like cylindrical co-ordinates on the sphere near the south pole.

We claim that a Hamiltonian flip (or period doubling) bifurcation takes place as μ passes through μ_*. Here $\lambda = \lambda_* \neq \pm 1, 6$ is fixed and $(\lambda_*, \mu_*) \in B \cup F$.

The classical scenario is that of a periodic orbit losing its stability, giving rise to a stable periodic orbit of twice the period, cf. [43]. For the full normal form $\bar{H}_\varepsilon$ in three degrees of freedom this translates to an invariant 2-torus switching from normal ellipticity to normal hyperbolicity, with a normally elliptic invariant 2-torus branching off that has one of its internal frequencies halved.

For the present $\mathbb{Z}_2$-symmetric one-degree-of-freedom system on U_μ this means that the equilibrium at $(0, 0, 1)$ undergoes a Hamiltonian pitchfork bifurcation. The standard planar model for such a bifurcation at the origin (as μ passes through μ_*) is

$$\tfrac{1}{2}\gamma_1 y^2 + \tfrac{1}{24}\gamma_2 x^4 + \gamma_3(\mu - \mu_*)x^2 \tag{27}$$

with non-zero constants $\gamma_1, \gamma_2, \gamma_3 \in \mathbb{R}$. The various possible signs yield four scenarios. If the ratio γ_2/γ_1 is negative, the newly born pair of equilibria is hyperbolic, so we expect $\gamma_2/\gamma_1 > 0$. Since the pair of elliptic equilibria ceases to exist for $|\mu| > |\mu_*|$, we expect $\gamma_3/\gamma_1 > 0$ when $\mu_* > 0$ and $\gamma_3/\gamma_1 < 0$ when $\mu_* < 0$.

Our aim is to find local co-ordinates near $(u, v, w) = (0, 0, 1)$ in which the dominant terms of $\mathcal{H}^\lambda$ assume the simple form (27). Showing that the pertinent coefficients are non-zero, and that the various signs are as described above then finishes the proof of Theorem 4.1.

Projecting U_μ to the (u, v) plane yields a chart around $(0, 0, 1)$ from which we start our computations. Note that these are not symplectic co-ordinates as

$$\{u, v\} = \frac{w^2 + w - 2\mu^2}{\sqrt{(w + 1)^2 - 4\mu^2}}. \tag{28}$$

However, this could be remedied by rescaling time and does not affect the values of $\gamma_1, \gamma_2, \gamma_3$. We use (26) to express $w = w_\mu(u, v)$ and obtain

$$H_{\lambda,\mu}(u, v) := \mathcal{H}^\lambda(u, v, w_\mu(u, v)). \tag{29}$$

Because of the reversibility and the $\mathbb{Z}_2$-symmetry only the terms u^2, v^2, u^4, u^2v^2, v^4 in the 4-jet will have non-zero coefficients. Omitting constant terms, the 2-jet of $H_{\lambda,\mu}$ reads

$$H^{2\text{-jet}}_{\lambda,\mu}(u, v) = \lambda(1 - 6\lambda)\frac{u^2 - v^2}{2} - \frac{\lambda(6 - \lambda)}{\sqrt{1 - \mu^2}}\frac{u^2 + v^2}{2}.$$

This shows that the origin is a parabolic equilibrium when $(\lambda, \mu) = (\lambda_*, \mu_*) \in B \cup F$. Indeed, for $\lambda_* \in]1, 6[$ we have

$$H^{2\text{-jet}}_{\lambda_*,\mu_*}(u, v) = \lambda_*(1 - 6\lambda_*)u^2,$$

while for $\lambda_* > 6$ or $\lambda_* < -1$ we have

$$H^{2\text{-jet}}_{\lambda_*,\mu_*}(u, v) = -\lambda_*(1 - 6\lambda_*)v^2.$$

This gives the coefficient γ_1 we look for,

$$\gamma_1 = \pm\lambda_*(1 - 6\lambda_*) = \frac{-\lambda_*(6 - \lambda_*)}{\sqrt{1 - \mu_*^2}}$$

and

$$\gamma_3 = \frac{\mathrm{d}}{\mathrm{d}\mu}\frac{-\lambda_*(6 - \lambda_*)}{\sqrt{1 - \mu^2}}\bigg|_{\mu=\mu_*} = \frac{-\mu_*\lambda_*(6 - \lambda_*)}{\sqrt{1 - \mu_*^2}^3}$$

leads in all cases to $(\gamma_3/\gamma_1) = (\mu_*/(1 - \mu_*^2))$ which bears the sign of μ_* as expected.

To prove that $(\gamma_2/\gamma_1) > 0$ we have to compute the pertinent term of order 4. The 4-jet of $H_{\lambda,\mu}$ has the additional term

$$-\frac{5 - 5\lambda^2 - \mu^2(5 - 12\lambda - 3\lambda^2)}{16(1 - \mu^2)^2}(u^2 + v^2)^2 \tag{30}$$

and the coefficient turns for $(\lambda, \mu) = (\lambda_*, \mu_*) \in B \cup F$ into

$$\gamma_2 = -\frac{15(1 - 6\lambda_*)^2(1 - \lambda_*^2)(2 - 5\lambda_*)}{16(6 - \lambda_*)^3}.$$

Hence, γ_2 is negative for $\lambda_* \in]1, 6[$ and positive when $\lambda_* > 6$ or $\lambda_* < -1$, yielding in all cases $(\gamma_2/\gamma_1) > 0$. This concludes the proof.

We end this section with a short survey of the various cases of structurally stable 1-parameter families of one-degree-of-freedom systems. The relevant information is contained in the set Σ_λ of critical values of the mapping

$$(\mu, \mathcal{H}^\lambda) : V_\mu \to \mathbb{R}^2 \tag{31}$$

which is closely related to the energy–momentum mapping $\mathcal{EM} = (\bar{H}, L, N) : T^*\mathbb{R}^3 \to \mathbb{R}^3$ of the full normal form in three degrees of freedom. Qualitative changes of Σ_λ only occur

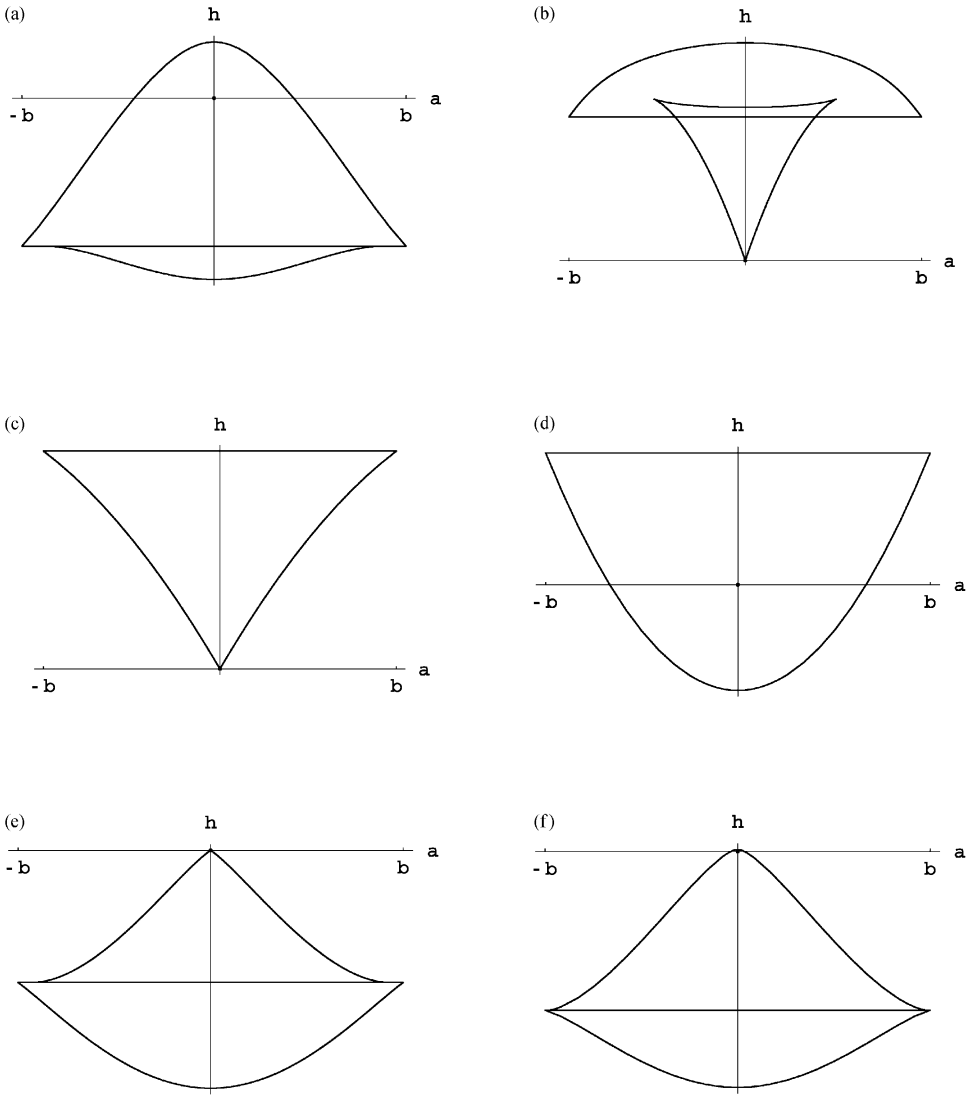

Fig. 5. The set Σ_λ of critical values (μ, h) of (31) for the various structurally stable cases, with λ in the six sets $]6, \infty[\cup] - \infty, -1[$, $] - 1, 0[$, $]0, \frac{1}{2}[$, $]\frac{1}{2}, 1[$, $]1, \frac{5}{2}[$ and $]\frac{5}{2}, 6[$. Note that the origin $(\mu, h) = (0, 0)$ is always contained in Σ_λ.

as λ passes through one of the exceptional values $-1, 0, \frac{1}{2}, 1, \frac{5}{2}, 6$. For each structurally stable case the set of critical values of $(\mu, \mathcal{H}^\lambda)$ is given in Fig. 5.

Periodic orbits consist of regular points of $(\mu, \mathcal{H}^\lambda)$, so all elements of Σ_λ correspond to equilibria. The lines in Σ_λ parametrise centres and saddles, in particular the straight line parametrises the singular equilibria $(0, 1)$ in V_μ. The corners at $\mu = \pm 1$ stand for

the equilibria in $V_{\pm 1} = \{(0, 1)\}$ while the singular equilibrium $(0, 0)$ in V_0 gives rise to a corner if it is a centre and to an isolated point if it is a saddle. Where a further curve touches the straight line the equilibrium at $(0, 1)$ bifurcates, and the centre–saddle bifurcations are represented by the two cusps in Fig. 5b. The double points in that figure just mean that there two centres have the same energy, so this has no dynamical consequences. Since extrema of $\mathcal{H}^\lambda$ are assumed in centres, it is straightforward to decide which of the lines parametrise saddles. As already remarked the parameter value "$\lambda = \infty$" can easily be incorporated again, in fact it is "obviously missing" in $]6, \infty[\cup] - \infty, -1[$. We discuss in the next section how isolated values of (31) give rise to monodromy.

4.5. The exceptional cases

If $\lambda = \lambda_* \in \{-1, 0, \frac{1}{2}, 1, \frac{5}{2}, 6\}$ (fixed), then the dynamical behaviour of the 1-parameter family of one-degree-of-freedom systems defined by $\mathcal{H}^\lambda$ on V_μ may change under small perturbations. This is easily proven considering again the set Σ_λ of critical values of (31), see Fig. 6. Let us take the small perturbation defined by altering λ a little bit. Depending on whether λ gets increased or decreased, Σ_λ is changed to one of the two bordering cases depicted in Fig. 5. These two possible sets of critical values differ by themselves, so it is a priori clear that $\mathcal{H}^{\lambda_*}$ does not define a structurally stable family on V_μ.

An interesting question is now whether all possible qualitative behaviours attainable by small perturbations of the exceptional cases are already accounted for in the reduced normalised family (21). This would imply that a further addition of (axially symmetric) quartic potentials with sufficiently small coefficients would not alter the normalised dynamics, and that the same holds true for higher order potentials if one restricts to a neighbourhood sufficiently close to the origin.

4.5.1. The case $\lambda_* = 6$

The parabola p_6 defined by (23) has its minimum at $\tau_2 = 1$. For nearby values λ the slope of p_λ in $\tau_2 = 1$ is non-zero and eventually a Hamiltonian flip bifurcation occurs when this slope equals that of q_μ in $\tau_2 = 1$. This does not happen when $\lambda = 6$, here it is the equilibrium $(0, 1)$ in $V_{\pm 1}$ that bifurcates. When λ passes through $\lambda_* = 6$, the slope of p_λ in $\tau_2 = 1$ changes its sign. Consequently the family, parametrised by λ, of 1-parameter families of one-degree-of-freedom systems, all of which are parametrised by μ, is structurally stable when λ passes through 6. Let us analyse this in the following paragraphs.

The perturbations we allow do have to satisfy some conditions. The Hamiltonian structure should be respected and, thinking of perturbations of the second-order normal form $\bar{H}_\varepsilon$ in three degrees of freedom, the axial symmetry and the oscillator symmetry should both remain valid. A typical example we have in mind are higher order normal forms. As a result the perturbation can again be reduced to one degree of freedom with the same family of phase spaces V_μ and thus defines a small perturbation $\mathcal{K}$ of $\mathcal{H}^6$. For instance, the perturbed energy may explicitly depend on the distinguished parameter μ.

Let us first assume that the perturbation respects the reversible symmetry $\operatorname{Im}\tau_1 \mapsto -\operatorname{Im}\tau_1$ as well. This is the case for reversible perturbations in three degrees of freedom, in particular for higher order normal forms. Then $\mathcal{K}$ is even in $\operatorname{Im}\tau_1$, i.e. $\operatorname{Im}\tau_1$ only enters squared. Therefore, the equilibria remain on the meridian section $V_\mu \cap \{\operatorname{Im}\tau_1 = 0\}$ (since

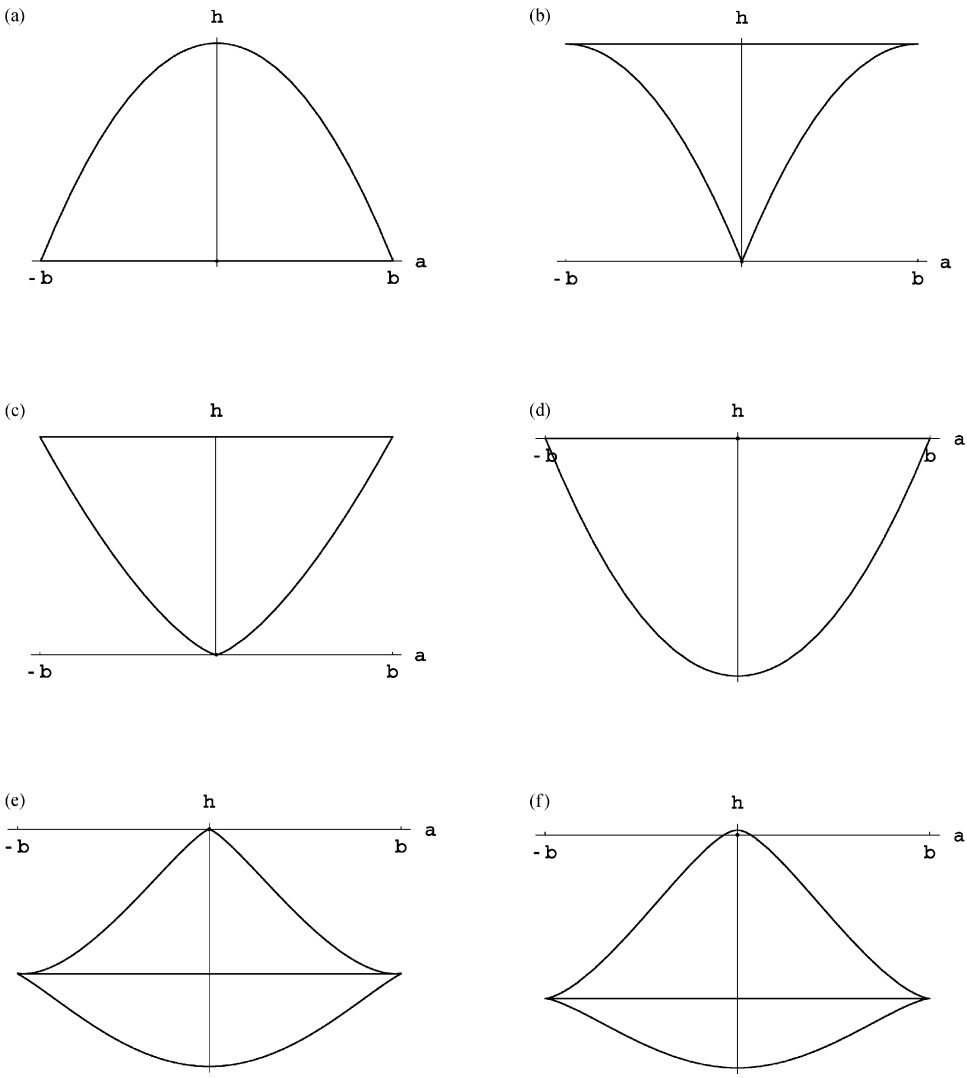

Fig. 6. The set Σ_{λ_*} of critical values (μ, h) of (31) for the exceptional cases $\lambda_* = -1, 0, \frac{1}{2}, 1, \frac{5}{2}, 6$.

$\mathcal{K}$ is close to $\mathcal{H}^6$). Thus, we merely have to replace p_6 by a function f parametrising the energy levels

$$\{\mathcal{K} = h\} \cap \{\mathrm{Im}\,\tau_1 = 0\} = \{\mathrm{Re}\,\tau_1 = f(\tau_2)\}.$$

The dynamical behaviour of the family of one-degree-of-freedom systems defined by $\mathcal{K}$ on V_μ is governed by the value of $f'(1)$. In case this value is positive (zero, negative), the dynamical behaviour is equivalent to that of the family defined by $\mathcal{H}^\lambda$ for $\lambda \in]\frac{5}{2}, 6[$ ($\lambda = 6$,

$\lambda > 6$). Here we use that $p_6''(0) = \frac{5}{6} > 0$ and that f is a small perturbation of p_6, whence f behaves like a parabola near $\tau_2 = 1$.

Let $\hat{\tau}_2(\lambda)$ denote the position of the extremum of p_λ. Since $(\mathrm{d}/\mathrm{d}\lambda)\hat{\tau}_2(6) = \frac{6}{175} > 0$, the family $\mathcal{H}^\lambda$ of families of one-degree-of-freedom systems defined on V_μ versally unfolds the bifurcation occurring at $\lambda = 6$.

In case the reversibility is destroyed one can use the implicit mapping theorem to show that all equilibria lie on a curve through $\tau = (0, 1)$ (and also through $\tau = (0, 0)$ if $\mu = 0$) that is very close to the meridian section (22). The above argumentation still applies after a small transformation on V_μ that turns this curve into (22).

4.5.2. The case $\lambda_* = 0$

To prove that the passage through $\lambda = 0$ is degenerate we perturb the energy by adding $\delta \cdot \mathrm{Re}\,\tau_1$ (δ small) to it. Note that in this way all existing symmetries are respected. For $\delta \neq 0$ the energy levels are parabolic cylinders even when $\lambda = 0$, and again it is the relative position of the parabola within $\mathrm{Im}\,\tau_1 = 0$ to the contour of V_μ that governs the dynamics. At $\lambda = 0$ the extremum of the parabola is assumed in $\tau_2 = 1$, so we have the same dynamical behaviour as at $\lambda = 6$: for all $|\mu| < 1$ the equilibrium $(0, 1)$ is a saddle and $(0, 1) \in V_{\pm 1}$ bifurcates. For non-zero λ this induces Hamiltonian flip bifurcations with $(0, 1)$ becoming a centre again. Thus, the effect of the perturbative term $\delta \cdot \mathrm{Re}\,\tau_1$ is that the line D in Fig. 3 gets replaced by two curves of Hamiltonian flip bifurcations connecting $(\lambda, \mu) = (0, 1)$ and $(0, -1)$. Since δ is small, the strip between these curves will be quite narrow.

Now the original family (1) defines an integrable system for $\lambda = 0$ where (1) is in fact separable, consisting of a 2D harmonic oscillator and the 1D anharmonic oscillator

$$\tfrac{1}{2}p_3^2 + \tfrac{1}{2}\omega^2 x_3^2 + \tfrac{1}{3}\varepsilon x_3^3.$$

Consequently, the situation changes if one restricts to perturbations defined by higher order normal forms. Let us denote by $\mathcal{K}^\lambda$ such a perturbation of $\mathcal{H}^\lambda$. The normal form procedure affects only the (x_3, p_3) subsystem and higher order terms in the normal form become functions in $\frac{1}{2}(p_3^2 + \omega^2 x_3^2) = \tau_2 - 1$ (recall that we have scaled the total energy b of the harmonic oscillator to 1). In particular, additional terms involving τ_1 vanish for $\lambda = 0$ where the energy levels remain planes perpendicular to the τ_2 axis. As we have seen in the case $\lambda = \frac{1}{6}$ this is not sufficient to force the dynamics to be degenerate. But since the derivative of the energy with respect to τ_2 (still) vanishes at $\tau_2 = 1$, the plane passing through $\tau = (0, 1)$ is a degenerate "double plane" and the bifurcation that the system defined by $\mathcal{K}^\lambda$ on V_μ undergoes as λ passes through 0 remains the same as for the system defined by $\mathcal{H}^\lambda$; a centre and a saddle coalesce with the centre at $\tau = (0, 1)$. We refer to [54] for a detailed treatment of this bifurcation in the 2D Hénon–Heiles family along the lines sketched above. An additional complication in the present 3D case is that the line of centre–saddle bifurcations also terminates at $\lambda = 0$. But one readily checks that this is true for the bifurcation diagram defined by $\mathcal{K}^\lambda$ as well.

4.5.3. The cases $\lambda_* = \frac{1}{2}, \frac{5}{2}$

Comparing the phase portraits for values of (λ, μ) near $(\frac{1}{2}, 0)$ and $(\frac{5}{2}, 0)$ with those in the Lagrange top, see [11], we expect that a Hamiltonian Hopf bifurcation occurs. This is a

bifurcation of, e.g. an equilibrium in two degrees of freedom, where two pairs of imaginary eigenvalues meet and split off the imaginary axis, forming a quartet $\pm\gamma \pm \mathrm{i}\delta$. In this way a centre turns into a saddle as the parameter passes the bifurcation value. The bifurcating equilibrium is in 1 to -1 resonance.

The equilibrium at $\tau = (0, 0)$ stands for rectilinear "ellipses" where the whole energy is concentrated in the (x_3, p_3) subsystem. These are invariant under the whole S^1-action ϱ, and already the reduction of this axial symmetry mapped the (x_3, p_3) subsystem to the singular plane $\{(0, 0, \sigma_3)|\sigma_3 \in \mathbb{C}\}$ of the first reduced phase space. Therefore, we have to "unreduce" the axial symmetry if we want to study the bifurcations at $\tau = (0, 0)$ on a smooth phase space. In Section 4.4 it had been sufficient to pass to a 2:1 covering to achieve the same goal at $\tau = (0, 1)$.

It is preferable not to reconstruct the full system in three degrees of freedom, but only in two degrees of freedom with the oscillator symmetry still reduced. In this way we are led to $\mathbb{CP}^2$. Indeed, this is what one obtains by fixing the value b of L and reducing the oscillator symmetry directly on $T^*\mathbb{R}^3$, see [24,46,58] for more details. As this is a regular reduction this does not lead to singularities, $\mathbb{CP}^2$ is a smooth manifold.

To perform the reconstruction, one has to attach an S^1 to every point of the twice reduced phase spaces $V_{a,b}$ with the exception of the singular point $\tau = (0, 0)$ of $V_{0,b}$. In this way periodic orbits give rise to invariant 2-tori, while from the regular equilibria and from the equilibria at $\tau = (0, 1)$ one reconstructs periodic orbits. The equilibrium $\tau = (0, 0)$ remains an equilibrium for every $b > 0$. To obtain $\mathbb{CP}^2$ one has to take the union over $a \in [-b, b]$. The reader may wish to have a second look at Fig. 1 to get an idea how $\mathbb{CP}^2$ is foliated by these S^1-bundles over lemon and turnips. Note that the nodal-Lissajous variables provide local co-ordinates (g, ν, G, N) on $\mathbb{CP}^2$, but these are not defined in the equilibrium "reconstructed" from $\tau = (0, 0)$. In particular one can no longer consider the value a of N as a parameter of the system; the phase space variable N remains an integral of motion, though.

As we keep the oscillator symmetry reduced, the value b of L remains a (distinguished) parameter of the system. Hence, the second-order terms in the normal form (17) are still given by ωb, while a proper scaling makes b^2 a common factor of the fourth-order terms. Thus, for different values b of L one obtains equivalent flows on $\mathbb{CP}^2$, i.e. this parameter influences the (reduced) dynamics only through a global scaling of the time.

To prove that indeed a Hamiltonian Hopf bifurcation occurs as the external parameter λ passes through $\frac{1}{2}$ or $\frac{5}{2}$ one has to check that the pertinent transversality conditions are met, i.e. that certain higher order terms in the Taylor expansion of the Hamilton function about the equilibrium do not vanish, cf. [11,42]. This lies beyond the scope of the present paper (but see [31] for more details). Our conjecture is supported by the fact that, for λ near $\frac{1}{2}$ or $\frac{5}{2}$, the set $\Sigma = \bigcup \Sigma_\lambda$ of critical values of the energy–momentum mapping

$$\mathcal{EM} = (\bar{H}^\lambda, N) : \mathbb{CP}^2 \to \mathbb{R}^2$$

displays the typical structure of the Hamiltonian Hopf bifurcation of hyperbolic type, cf. Figs. 5 and 6.

As shown in [18], the hyperbolic equilibria coming from a Hamiltonian Hopf bifurcation always entail monodromy in the system, see also [11,48]. In the present situation the hyperbolic equilibria correspond to the isolated critical value $(0, 0)$ of $\mathcal{EM}$ in Figs. 5a, d,

f and 6f. The surrounding regular values stand for invariant 2-tori, and tracing a small loop in (μ, h) space around the origin defines a diffeomorphism on $\mathbb{T}^2$. The system is said to have monodromy if this diffeomorphism is not homotopic to the identity, see [11] for more details. In particular the bundle of maximal tori (the base space of which is given by the regular values in the image $\mathrm{im}(\mathcal{EM})$ of the energy–momentum mapping) is not a trivial bundle. On $\mathbb{CP}^2$ this is a 2-torus bundle, and in the full system on $T^*\mathbb{R}^3$ this is a 3-torus bundle. Hamiltonian Hopf bifurcations occurring at $\lambda_* = \frac{1}{2}, \frac{5}{2}$ imply such diffeomorphisms to be homotopic to

$$\begin{pmatrix} 1 & 1 \\ 0 & 1 \end{pmatrix} \quad \text{and} \quad \begin{pmatrix} 1 & 1 & 0 \\ 0 & 1 & 0 \\ 0 & 0 & 1 \end{pmatrix},$$

respectively.

4.5.4. The cases $\lambda_* = \pm 1$

In these cases the parabola (23) coincides for $\mu = 0$ with the contour (22) along the upper or lower arc, respectively. This makes it obvious that small perturbations can change the dynamical behaviour, and in fact for $\lambda_* = -1$ already the higher order normal forms break the degeneracy. This is the 3D Hénon–Heiles case, which has been proven in [58] to be algebraically non-integrable (see also [21,22] for a detailed study of this case). According to [19] the normal forms up to order 20 do not break the degeneracy at $\lambda_* = +1$, and we show below that this holds true for all higher order normal forms. As a consequence the behaviour near $\lambda = +1$ of the 1-parameter family of 1-parameter families defined by $\mathcal{H}^\lambda$ on V_μ is not altered by higher order normal forms. Thus the two exceptional values $\lambda_* = 0, 1$ for which (1) is integrable induce a degenerate behaviour shared by all normal forms.

The degeneracy of the 3D Hénon–Heiles case $\lambda_* = -1$ is already broken by the fourth-order normal form, and this raises the question whether *that* normal form is insensitive to small perturbations or at least to the perturbations defined by the normal forms of order 6 and higher. For instance, the results in [22,58] indicate that the curves B and C of Fig. 3 cease to touch and intersect instead, leading to an additional open region with one hyperbolic and three elliptic regular equilibria and a saddle at $\tau = (0, 1)$. However, the details of the refinement around $(\lambda, \mu) = (-1, 0)$ of Fig. 3 imposed by the normal form of order 4 are beyond the scope of the present paper.

4.5.5. Relation to the 2D Hénon–Heiles family

The degeneracies $\lambda_* = \pm 1$ manifest for $\mu = 0$. Let us have a closer look at the dynamics when the third component of the angular momentum vanishes. The points on the lemon V_0 represent all polar orbits, i.e. motions confined to some plane containing the x_3 axis. Here we recover the 2D Hénon–Heiles family. Correspondingly, we have already seen that the reduced phase space U_0 of the 1–1 resonance is a 2:1 cover of V_0. The reason is that we identified all ellipses that are mapped to each other under the axial S^1-action. In particular, those ellipses that differ by a π-rotation are represented by the same point on V_0, but by two different points on the 2:1 cover U_0.

The studies [10,45] of the second-order normal form of the 2D Hénon–Heiles family revealed at $\lambda_* = \pm 1$ great circles of equilibria (which doubly cover the upper and lower arc of (22), respectively). The parabolic equilibria occurring for $\lambda_* = \frac{1}{2}, \frac{5}{2}$ undergo Hamiltonian pitchfork bifurcations. These studies have been extended in [8] to the fourth-order normal form of the 2D Hénon–Heiles family. Let us report on the results obtained for the passage through $\lambda = 1$, translating them to the lemon V_0. We concentrate on sufficiently small $\varepsilon > 0$, whence all equilibria fulfil $\operatorname{Im} \tau_1 = 0$.

Starting with parameter values $\lambda \ll -1$, the flow on V_0 is as indicated in Fig. 3 on the line A. Both singular equilibria are saddles, and there are two regular centres. The (un)stable manifold of the saddle at $\tau = (0, 1)$ encircles the centre on the upper arc of the meridian section $\operatorname{Im} \tau_1 = 0$, while the (un)stable manifold of the saddle at $\tau = (0, 0)$ encircles the centre on the lower arc. When λ passes through a certain value $\lambda_1 < -1$, the saddle at $\tau = (0, 0)$ bifurcates: the stable and unstable manifold both emanate along the upper arc. For $\lambda > \lambda_1$ the singular equilibrium at $\tau = (0, 0)$ has turned into a centre, giving rise to a regular saddle on the upper arc. The (un)stable manifold of the saddle at $\tau = (0, 1)$ keeps encircling the centre on the upper arc while the (un)stable manifolds of the regular saddle encircle the singular centre and the regular centre on the lower arc.

As λ passes through $\lambda_2 := -1$, a global bifurcation occurs, the two saddles become connected by heteroclinic orbits. When $\lambda > -1$ the (un)stable manifold of the singular saddle encircles the regular centre on the lower arc, and the (un)stable manifolds of the regular saddle encircle the singular centre and the regular centre on the upper arc. While increasing λ the two regular equilibria on the upper arc approach each other and meet in a *transcritical bifurcation* when $\lambda = \lambda_3$. We will further comment on this in Section 5.3. There is a second *connection bifurcation* when λ passes through a certain value $\lambda_4 > \lambda_3$ and for $\lambda > \lambda_4$ the flow is equivalent to the one for $\lambda \in]\lambda_1, \lambda_2[$. The final bifurcation occurs at some $\lambda_5 \in]\lambda_4, 0[$ where the regular centre on the upper arc reaches the singular saddle and vanishes, while the singular equilibrium at $\tau = (0, 1)$ turns into a centre. When $\lambda \in]\lambda_5, 0[$ the flow is as indicated in Fig. 3. Both singular equilibria are centres, there is a regular saddle on the upper arc and a regular centre on the lower arc.

Hence, the simple reason for the degenerate second-order normal form $\mathcal{H}^{-1}$ is that a parabolic cylinder cannot touch the lemon V_0 at more than four isolated points. Passing to the double cover U_0, the five equilibria of the fourth-order normal form on V_0 give rise to the familiar eight equilibria of the reduced normalised 2D Hénon–Heiles system. The bifurcation values $\lambda_1, \lambda_3, \lambda_4, \lambda_5$ are functions of ε and tend to -1 as $\varepsilon \to 0$. Cotter [8] allows ε to be large and details a spectacular bifurcation diagram where the higher order terms start dominating the lower order terms in the fourth-order normal form. We remark that the bifurcation diagram in [22], which was obtained using nodal-Lissajous variables, has to be completed by the segment between E_0 and E_4 where the two saddles are connected by heteroclinic orbits.

On this basis one may speculate on the refinement of the bifurcation diagram around $(\lambda_*, \mu_*) = (-1, 0)$, see Fig. 3, if one passes to the fourth-order normal form. The curves B and C will intersect, forming a new region which includes the point $(-1, 0)$. This region contains two lines (or one line passing twice through the λ axis) of connection bifurcations, one of which passes exactly through $(-1, 0)$. It is not yet clear how to continue the transcritical bifurcation. The line A ends where C intersects the λ axis. Thus, as λ passes

through that point, the singular equilibrium at $\tau = (0, 0)$ turns from a saddle to a centre and two curves of centre–saddle bifurcations emanate. We remark that this is typical for a Hamiltonian Hopf bifurcation of elliptic type, cf. [42].

We end this section showing that the degeneracy of the system at $(\lambda_*, \mu_*) = (1, 0)$ persists through all orders of the normal form. This may be done in two degrees of freedom, e.g. putting $(x_2, p_2) = (0, 0)$ whence $\mu = 0$. As noted in [2] the case $\lambda_* = 1$ of the 2D Hénon–Heiles family is separable; the rotation

$$x_1 = \frac{\xi_1 - \xi_2}{\sqrt{2}}, \qquad x_3 = \frac{\xi_1 + \xi_2}{\sqrt{2}}, \qquad p_1 = \frac{\eta_1 - \eta_2}{\sqrt{2}}, \qquad p_3 = \frac{\eta_1 + \eta_2}{\sqrt{2}}$$

turns (1) at $(x_2, p_2) = (0, 0)$ into the sum

$$H_\varepsilon(\xi, \eta) = \tfrac{1}{2}(\eta_1^2 + \eta_2^2) + \tfrac{1}{2}\omega^2(\xi_1^2 + \xi_2^2) + \tfrac{1}{3}\sqrt{2}\varepsilon(\xi_1^3 + \xi_2^3) \tag{32}$$

of two uncoupled 1D anharmonic oscillators. Following [19] we note that the Hopf variables u, v, w on the 2:1 cover $U_0 = \{(u, v, w) \in \mathbb{R}^2 | u^2 + v^2 + w^2 = 1\}$ of the lemon V_0 are expressed in ξ, η as

$$u = \frac{1}{4\omega}(\eta_1^2 - \eta_2^2 + \omega^2(\xi_1^2 - \xi_2^2)), \qquad v = \frac{1}{2}(\xi_1\eta_2 - \xi_2\eta_1),$$
$$w = \frac{1}{2\omega}(\eta_1\eta_2 + \omega^2\xi_1\xi_2).$$

For higher order normal forms it is not longer possible to scale the value b of $L = (1/\omega)H_0$ away, so we now incorporate it again writing

$$u^2 + v^2 + w^2 = \frac{b^2}{4}, \quad b = \frac{1}{2\omega}(\eta_1^2 + \eta_2^2 + \omega^2(\xi_1^2 + \xi_2^2)).$$

As the normal forms of the anharmonic oscillator $\frac{1}{2}\eta^2 + \frac{1}{2}\omega^2\xi^2 + \frac{1}{3}\sqrt{2}\varepsilon\xi^3$ are functions in $\frac{1}{2}(\eta^2 + \omega^2\xi^2)$, the normal forms of (32) only depend on b and u. Since it is possible to pass to V_0 by means of (24), every normal form is in fact a function in b and u^2. As a consequence the meridian $u = 0$ of U_0 consists of equilibria. The 2:1 covering (24) maps this meridian to the lower arc $\operatorname{Im}\tau_1 = 0$, $\operatorname{Re}\tau_1 \leq 0$ of V_0.

Remark. In 1-parameter families of Hamiltonian systems that are integrable at a certain parameter value one often encounters a circle of equilibria. In [7] this is termed a *Birkhoff bifurcation* and conditions are studied where this is a generic phenomenon. In the present situation we encounter the further degeneracy that the circle of equilibria always coincides with the meridian $u = 0$ on U_0. Therefore, it projects on V_0 only to the lower arc and not to a whole circle of equilibria as well.

5. Implications for the original system

In the previous section we described the dynamical behaviour of the various one-degree-of-freedom systems defined by the normal form, their dependence on the distinguished parameters a, b and where these families change their behaviour as the external parameters α, β

are varied. To obtain information on the "original flow", defined by (1), we use that (in appropriate co-ordinates, given by the normalisation procedure) H_ε is an ε^4-small perturbation of $\bar{H}_\varepsilon$. For fixed ratio $\beta/\alpha \notin \{-1, 0, \frac{1}{2}, 1, \frac{5}{2}, 6\}$ the family $\bar{H}_\varepsilon^{a,b}$ of one-degree-of-freedom systems is insensitive to small perturbations. To use this we have to reconstruct the dynamics of $\bar{H}_\varepsilon$ on a phase space where H_ε is defined as well, i.e. to two or three degrees of freedom. It is preferable to carry out the perturbation analysis in two degrees of freedom. This allows for strong results because 2-tori become periodic orbits and thus accessible to the implicit mapping theorem, while those maximal tori that survive, parametrised by a Cantor set, divide the energy shells, leading to results on (dynamical) stability. In Section 5.4 the dynamics of H_ε is reconstructed to three degrees of freedom.

5.1. Reconstruction to two degrees of freedom

Our first goal is to reconstruct the dynamics of $X_{\bar{H}_\varepsilon}$ on $\{\sigma \in \mathbb{C}^3 | P(\sigma) = 0, \operatorname{Re}\sigma_2 \geq 0\}$. To this end we have to attach an S^1 to every point of the twice reduced phase space $V_{a,b}$. Where the nodal-Lissajous variables are defined, i.e. when $|N| < G < L$, this S^1 is parametrised by the angle ℓ. In this way the periodic orbits of $X_{\bar{H}_\varepsilon^{a,b}}$ give rise to invariant 2-tori, and the equilibria lead to periodic orbits of $X_{\bar{H}_\varepsilon}$. Thus, the 3D invariant subvarieties $N^{-1}(a) \cap L^{-1}(b)$ of $P^{-1}(0)$ become ramified 2-torus bundles. The regular fibres form families of 2-torus which are separated by the stable and unstable manifolds of hyperbolic periodic orbits (or, occasionally, of parabolic periodic orbits) and shrink down to elliptic periodic orbits with $\sigma \neq 0$. The situation near the periodic orbit $\sigma(t) = (\sigma_1(t), 2\omega(b + \mathrm{i}a), 0)$ (with $|\sigma_1(t)| = 2\omega\sqrt{b^2 - a^2}$) of $X_{\bar{H}_\varepsilon}$ is more involved, reflecting the 2–1 resonance. As $a \to \pm b$ this periodic orbit shrinks to an equilibrium, here the whole "ramified torus bundle" $\{\sigma \in \mathbb{C}^3 | P(\sigma) = 0, L(\sigma) = b, N(\sigma) = \epsilon b\}$, $\epsilon = \pm 1, b \geq 0$ consists of this single point.

We also have to understand how the invariant level sets fit together to form the (first reduced) phase space $\{\sigma \in \mathbb{C}^3 | P(\sigma) = 0, \operatorname{Re}\sigma_2 \geq 0\}$. We can collect the relevant information in one picture, the set Σ of critical values of

$$(\bar{H}_\varepsilon, N, L) : \{\sigma \in \mathbb{C}^3 | P(\sigma) = 0, \operatorname{Re}\sigma_2 \geq 0\} \to \mathbb{R}^3.$$

Note that the lift of this mapping to $T^*\mathbb{R}^3$ is the energy–momentum mapping of $\bar{H}_\varepsilon$ on $T^*\mathbb{R}^3$. Here we have suppressed the dependence of Σ on the external parameters α, β in the notation. The critical values are symmetric with respect to the reflection $a \mapsto -a$. For a fixed value b of L the slice Σ_b of critical values is depicted in Figs. 5 and 6, depending on the ratio $\lambda = \beta/\alpha$. The scaling (20) shows that the whole set Σ of critical values is a cone over Σ_b, distances in the a-direction increase linearly with b as does the minimal energy on Σ_b, while the maximal energy on Σ_b behaves like $b + \varepsilon b^2$. In particular also a level set $\bar{H}_\varepsilon = h$ of Σ is diffeomorphic to the depicted b-slice.

5.2. The perturbation analysis

Our aim is to understand the dynamics of the perturbation (1) of the isotropic harmonic oscillator. To this end we consider H_ε as a perturbation of its normal form $\bar{H}_\varepsilon$. Being now

in two degrees of freedom, the latter becomes sensitive to small perturbations, e.g. ceasing to be integrable. However, the main features of the flow of $X_{\bar{H}_\varepsilon}$ are persistent and thus in particular present in the flow of X_{H_ε} as well.

First we use that the set $\{(0,0,\sigma_3)|\sigma_3 \in \mathbb{C}\}$ of singularities of $P^{-1}(0)$ is necessarily X_{H_ε}-invariant. The intersections with the energy levels $\{H_\varepsilon = h\}$ correspond to the solutions of the equations of motion

$$\dot{\sigma}_1 = 0, \qquad \dot{\sigma}_2 = 0, \qquad \dot{\sigma}_3 = -\omega \mathrm{i}\sigma_3 - \frac{\varepsilon\alpha \mathrm{i}}{4\omega^2}(\sigma_3 + \bar{\sigma}_3)^2 \tag{33}$$

which essentially describe 1D anharmonic oscillations around the origin.

We now turn to the regular subset $\{\sigma \in \mathbb{C}^3 | P(\sigma) = 0, \operatorname{Re}\sigma_2 > 0\}$. Theorem 3.1 of [12] yields the inequality

$$\|H_\varepsilon \circ \varphi_\varepsilon - \bar{H}_\varepsilon\|_{A(h)} \leq \Gamma(h) \cdot \varepsilon^4$$

for sufficiently small ε. Here φ_ε is the normalising transformation, $\|\cdot\|_{A(h)}$ denotes the supremum norm on the union $A(h)$ of the energy shells $\{H = h'\}$ with $h' \leq h$, and $\Gamma(h)$ is a constant that only depends on h (and not on ε).

We look for persistence of the dynamics of $X_{\bar{H}_\varepsilon}$ on the energy shells. To apply the implicit mapping theorem to the persistence of elliptic and hyperbolic periodic orbits we need estimates $|H_\varepsilon \circ \varphi_\varepsilon - \bar{H}_\varepsilon| < c\varepsilon^2$ on some neighbourhood, with a constant c independent of ε. Such estimates are true for $\varepsilon^2 < c/\Gamma(h)$. The stable and unstable manifolds of hyperbolic periodic orbits will no longer coincide, but are expected to split.

In what concerns occurring parabolic periodic orbits these are, for $\lambda \neq \pm 1$, all involved in (periodic) centre–saddle bifurcations or Hamiltonian flip bifurcations that are versally unfolded by the distinguished parameter a. As shown in [43] the same estimate $|H_\varepsilon \circ \varphi_\varepsilon - \bar{H}_\varepsilon| < c\varepsilon^2$, with a possibly smaller constant c, yields the persistence of these bifurcations.

The persistence of most invariant 2-tori follows from [3,5]. The crucial point is the asymptotic behaviour of the frequency mapping as $\varepsilon \to 0$. With respect to suitably chosen actions (L, I) the frequency vector is of the form

$$D\bar{H}_\varepsilon(L, I) = \begin{pmatrix} \omega \\ 0 \end{pmatrix} + \mathrm{O}(\varepsilon^2).$$

To ensure the persistence of a large Cantor set of 2-tori on each energy shell we need that the determinant

$$\det \begin{pmatrix} D^2\bar{H}_\varepsilon & D\bar{H}_\varepsilon \\ D\bar{H}_\varepsilon & 0 \end{pmatrix} = -\omega^2 \frac{\partial^2 \bar{H}_\varepsilon}{\partial I^2} + \mathrm{O}(\varepsilon^4) \tag{34}$$

is bounded from below by $\varepsilon^2\kappa$, with some $\kappa \neq 0$. To show that $(\mathrm{d}/\mathrm{d}(\varepsilon^2))(\partial^2\bar{H}_\varepsilon/\partial I^2)$ is non-zero at $\varepsilon = 0$, we remark that the reduced system $X_{\bar{H}_\varepsilon^{a,b}}$ on $V_{a,b}$ depends on ε only through a global multiplication by ε^2. Furthermore, the frequency $\partial\bar{H}_\varepsilon/\partial I$ is an analytic function, so it suffices to show that this function is not constant. In case the axially reduced normal form $\bar{H}_\varepsilon$ has hyperbolic periodic orbits, the frequency $\partial\bar{H}_\varepsilon/\partial I$ converges to zero upon approaching a separatrix. Where there are no hyperbolic periodic orbits, we use that

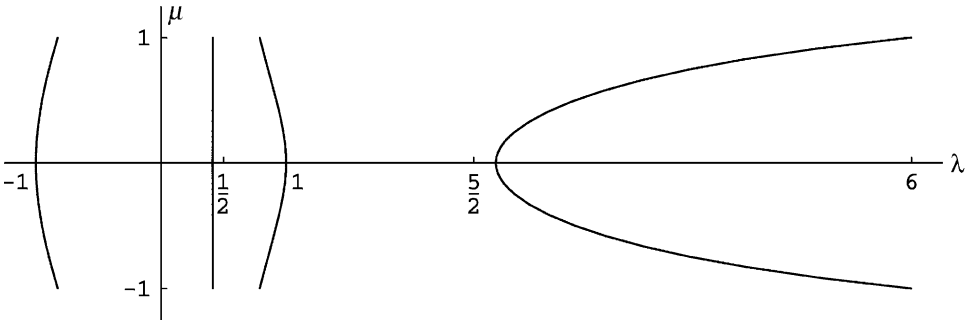

Fig. 7. The roots of (35). The line passing left of $\lambda = \frac{1}{2}$ is not a straight line, but has its unique left-most point on the λ-axis.

the frequency $\partial \bar{H}_\varepsilon / \partial I$ varies upon approaching an elliptic periodic orbit reconstructed from $\tau = (0, 1)$. To this end we show below that the second Birkhoff coefficient of $(u, v, w) = (0, 0, 1)$ on the double cover U_μ of V_μ does not vanish. Both argumentations show that $\partial \bar{H}_\varepsilon / \partial I$ is not constant. Extracting some neighbourhood of the isolated zeros of $\partial^2 \bar{H}_\varepsilon / \partial I^2$ we get the necessary lower bound $\varepsilon^2 \kappa$ of the determinant (34).

Applying the normalisation procedure of Section 3 near an elliptic equilibrium of a one-degree-of-freedom system, one obtains suited symplectic co-ordinates (p, q) in which the Hamilton function reads

$$\sum_{k=0}^{n} b_k (p^2 + q^2)^k + \text{higher order terms.}$$

The scalar b_k in this Birkhoff polynomial is the kth *Birkhoff coefficient*, cf. [4]. Note that b_k can be computed from the $2k$-jet of the Hamilton function in the elliptic equilibrium.

Starting our computation from (29), we have to take into account that (u, v) are not symplectic co-ordinates, but have Poisson bracket (28). A straightforward way to obtain $b_2(\lambda, \mu)$ is to normalise the vector field (instead of normalising the Hamilton function). The relevant factor of $b_2(\lambda, \mu)$ is

$$\begin{aligned} &6\lambda(6-\lambda)(1-6\lambda)^2 + 2(6-\lambda)^2(5-12\lambda-3\lambda^2) \\ &\quad +(1-\mu^2)(1-6\lambda)^2(5-12\lambda-3\lambda^2) \end{aligned} \tag{35}$$

and vanishes for $(\lambda, \mu) \in \mathbb{R} \times [-1, 1]$ only on the lines depicted in Fig. 7. Note that the line passing right to $\lambda = \frac{5}{2}$ is irrelevant as the periodic orbit is hyperbolic for these values of (λ, μ).

We focus on $\lambda = \lambda_* \in]0, 1[$ as there are 1-parameter families of hyperbolic periodic orbits for the other values of λ. Our two-degrees-of-freedom systems are parametrised by the value a of N. The elliptic periodic orbits reconstructed from $\tau = (0, 1)$ form a 1-parameter family parametrised by b. Thus, to $a \neq 0$ we may always find $b > 0$ such that $(\lambda, \mu) = (\lambda_*, (a/b))$ is not a root of (35). When $\lambda_* = 0.413\ldots$ and $a = 0$ we cannot avoid that (35) vanishes. To prove that $(\partial \bar{H}_\varepsilon / \partial I) \neq$ const. in this case, we computed the

second Birkhoff coefficient of $(u, v, w) = (0, 0, -1)$ on the double cover U_0 of V_0, which is non-zero.

Alternatively, one could use the nodal-Lissajous variables and put (15) in Birkhoff normal form around $G = |a|$. Indeed, (g, G) doubly cover V_μ (for $\mu \neq 0$) and provide "symplectic polar co-ordinates" around the regularised point $(u, v, w) = (0, 0, 1)$ on U_μ, i.e. the local co-ordinates (x, y) defined by

$$x = \sqrt{2(G - |a|)} \sin g, \qquad y = \sqrt{2(G - |a|)} \cos g$$

satisfy $\{x, y\} = 1$. A linear symplectic change $(x, y) \mapsto (q, p)$ puts the quadratic part of $\bar{H}_\varepsilon$ into normal form $b_1(p^2 + q^2)$. Since $\{q, p\} = 1$ one can normalise the Hamilton function itself to obtain b_2. While the concrete expression obtained this way may differ from (35), the set of (λ, μ) where "the" second Birkhoff coefficient vanishes has an intrinsic meaning and does not depend on the co-ordinates used to calculate it. It turns out that the expressions derived from (29) are less involved, but starting from (15) one can apply standard routines, i.e. it is not necessary to write special programs when doing the computations by machine.

Since we perform the perturbation analysis in two degrees of freedom, the energy shells are 3D and are divided by the 2D invariant tori. This leads to global (dynamical) stability results whenever the second Birkhoff coefficient is non-zero. Excluding a small strip around the left three lines of Fig. 7, the elliptic periodic orbits reconstructed from $\tau = (0, 1)$ are density points of the surrounding families of persistent invariant 2-tori.

To compute the second Birkhoff coefficients of the regular centres of the reduced system $X_{\bar{H}_\varepsilon^{a,b}}$ on $V_{a,b}$ we use the local co-ordinates (γ, Γ). We remark that these are not defined on the upper arc of the lemon and in the points $\Gamma = \frac{1}{2}b$ (the latter points are equilibria exactly for the 3D Hénon–Heiles case). The expressions of the second Birkhoff coefficients become very large and we have checked numerically that they do not vanish. Hence, these elliptic periodic orbits are dynamically stable. For the elliptic periodic orbits in the singular set $\{(0, 0, \sigma_3) | \sigma_3 \in \mathbb{C}\}$ this holds true as well since they constitute the limit as $a \to 0$ of regular elliptic periodic orbits.

This applies mutatis mutandis to the centres of $\bar{H}_\varepsilon$ at $\sigma = (0, |a| + \mathrm{i}a, 0)$, $a \in \mathbb{R}$. Here the energy takes the absolute value $b = |a|$ of the angular momentum, and since the axial symmetry is still reduced, these equatorial circular orbits correspond to equilibria on the first reduced phase space $\{\sigma \in \mathbb{C}^3 | P(\sigma) = 0, \operatorname{Re}\sigma_2 \geq 0\}$.

5.3. *Periodic orbits*

From [46] we know that the full three-degrees-of-freedom system X_{H_ε} has (at least) three families of periodic solutions emanating from the central equilibrium in 1–1–1 resonance. These are the vertical oscillations (33) and the horizontal circular orbits which reduce to equilibria $\hat{\sigma}$ in two degrees of freedom.

Let us directly compute the equilibria $\hat{\sigma}$ on the first reduced phase space to which the centres $\sigma = (0, |a| + \mathrm{i}a, 0)$ of $\bar{H}_\varepsilon$ are perturbed to. For $a \neq 0$ the co-ordinates $(\operatorname{Re}\sigma_1, \operatorname{Im}\sigma_1, \operatorname{Re}\sigma_3, \operatorname{Im}\sigma_3)$ provide a global chart of the invariant manifold $\{N = a\}$.

The symplectic structure is given by

$$\{\mathrm{Re}\,\sigma_1, \mathrm{Im}\,\sigma_1\} = 4\omega\sqrt{4\omega^2a^2 + (\mathrm{Re}\,\sigma_1)^2 + (\mathrm{Im}\,\sigma_1)^2}, \qquad \{\mathrm{Re}\,\sigma_3, \mathrm{Im}\,\sigma_3\} = \omega,$$
$$\{\sigma_1, \sigma_3\} = 0$$

and the equations of motion obtained from $H_\varepsilon(\sigma_1, \sigma_3)$ are

$$\frac{\mathrm{d}}{\mathrm{d}t}\mathrm{Re}\,\sigma_1 = 2\omega\,\mathrm{Im}\,\sigma_1 + \frac{2\beta\varepsilon}{\omega^2}\mathrm{Im}\,\sigma_1\mathrm{Re}\,\sigma_3,$$
$$\frac{\mathrm{d}}{\mathrm{d}t}\mathrm{Im}\,\sigma_1 = -2\omega\mathrm{Re}\,\sigma_1 - \frac{2\beta\varepsilon}{\omega^2}(\mathrm{Re}\,\sigma_1 + \sqrt{4\omega^2a^2 + (\mathrm{Re}\,\sigma_1)^2 + (\mathrm{Im}\,\sigma_1)^2})\mathrm{Re}\,\sigma_3,$$
$$\frac{\mathrm{d}}{\mathrm{d}t}\mathrm{Re}\,\sigma_3 = \omega\mathrm{Im}\,\sigma_3,$$
$$\frac{\mathrm{d}}{\mathrm{d}t}\mathrm{Im}\,\sigma_3 = -\omega\mathrm{Re}\,\sigma_3 - \frac{\alpha\varepsilon}{\omega^2}(\mathrm{Re}\,\sigma_3)^2 - \frac{\beta\varepsilon}{2\omega^2}(\mathrm{Re}\,\sigma_1 + \sqrt{4\omega^2a^2+(\mathrm{Re}\,\sigma_1)^2+(\mathrm{Im}\,\sigma_1)^2}).$$

The equilibria $(\hat\sigma_1, \hat\sigma_3)$ are given by

$$\mathrm{Im}\,\hat\sigma_1 = 0, \qquad \mathrm{Im}\,\hat\sigma_3 = 0, \qquad \mathrm{Re}\,\hat\sigma_3 = \frac{\omega\mathrm{Re}\,\hat\sigma_1}{4a^2\beta\varepsilon}(\mathrm{Re}\,\hat\sigma_1 - \sqrt{4\omega^2a^2 + (\mathrm{Re}\,\hat\sigma_1)^2}), \tag{36a}$$

where $\mathrm{Re}\,\hat\sigma_1$ is the unique solution near zero of

$$\mathrm{Re}\,\hat\sigma_1 = 2(\mathrm{Re}\,\hat\sigma_3)^2\left(1 + \frac{\alpha\varepsilon}{\omega^3}\mathrm{Re}\,\hat\sigma_3\right). \tag{36b}$$

As $\beta \to 0$ these expressions tend to $\hat\sigma_1 = 0$, $\hat\sigma_3 = 0$. According to Lyapunov's centre theorem, see [1], there originates a 1-parameter family of periodic orbits to each normal frequency of (36a,b) for which the other frequency is not an integer multiple of that frequency. Note that the two frequencies have an integer ratio if and only if the centre (36a,b) is in 2–1 resonance. In the separable case $\beta = 0$ this happens for all non-zero values of a.

There are further centres in 2–1 resonance. Linearising the equations of motion around (36a,b) yields a characteristic polynomial $\chi^4 + p\omega^2\chi^2 - q\omega^4$ with roots $\chi^2_\pm = -\frac{1}{2}p\omega^2 \pm \frac{1}{2}\omega^2\sqrt{p^2+4q}$ and the centre is in 2–1 resonance when $\chi^2_- = 4\chi^2_+$. Here the coefficients p and q depend on $\omega, a, \alpha, \beta, \varepsilon$ through $4\omega^2a^2$, $\beta\varepsilon/\omega^3$ and β/α. Again we write $\lambda = (\beta/\alpha)$. Then the above equation reads $a = \pm A(\lambda)$ with

$$A(\lambda) = \frac{10\omega^5(17-32\lambda)(1-\lambda)(6-\lambda)\sqrt{4-33\lambda+54\lambda^2}}{\varepsilon^2\lambda(4-93\lambda+64\lambda^2)^{5/2}} \tag{37}$$

which we only define for

$$\lambda \in]\tfrac{1}{128}(93+\sqrt{7625}), 6[, \tag{38}$$

cf. Fig. 8. Indeed, to obtain (37) we had to get rid of several square roots, leading to spurious solutions. The limit $\lim_{\lambda\to 6}A(\lambda) = 0$ reflects that the centres $(\hat\sigma_1, \hat\sigma_3) = (0, 0)$ of the normal form $\bar H_\varepsilon$ are in 2–1 resonance exactly when $\lambda = 6$ or $\lambda = 0$.

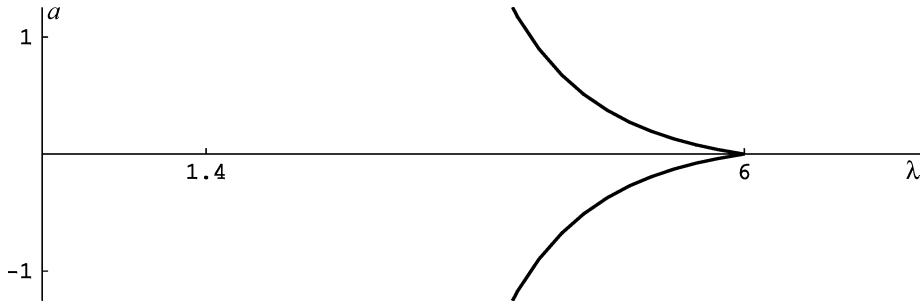

Fig. 8. The curves $a = \pm A(\lambda)$ for $\omega = \frac{1}{2}$ and $\varepsilon = 10^{-2}$.

Recall that ε measures how close we are to the origin (in three degrees of freedom), i.e. how valid the information provided by the normal form $\bar{H}_\varepsilon$ is. The expression (37) is derived from H_ε and therefore meaningful for all ε. Note that the 2–1 resonant centres have energies $2\omega b = 2\omega A(\lambda)$. Hence, even for very small ε we obtain a large energy when λ approaches the left boundary of (38). This defines a smaller interval $]\lambda_*, 6[$ of λ-values for which there is a 2–1 resonant centre in the region of validity of the normal form $\bar{H}_\varepsilon$. To study the dynamics near the 2–1 resonant centres when $\lambda < \lambda_*$ one should not work with $\bar{H}_\varepsilon$, but normalise H_ε with respect to the 2–1 resonant centres.

There are further rectilinear solutions next to (33). To compute these we make the ansatz

$$\tilde{\sigma} = ((\gamma + \mathrm{i}\omega\dot{\gamma})^2 d, (\gamma^2 + \omega^2\dot{\gamma}^2)d, (\gamma + \mathrm{i}\omega\dot{\gamma})c)$$

whence $d \geq 0$ (because one of the relations constraining (3) is $\mathrm{Re}\,\sigma_2 \geq 0$). For $d = 0$ this is the vertical rectilinear solution (33), while for $d > 0$ this corresponds to a whole S^1-family of rectilinear solutions with "directions" $\tan\theta = (c/\sqrt{d})$. A necessary condition for $\tilde{\sigma}$ to solve the equations of motion is then

$$\omega^2\varepsilon\gamma^3 cd(\alpha c^2 + \beta d - 2\beta c^2) = 0$$

and for $d \neq 0$ the function $\gamma = \gamma(t)$ is a solution of

$$\ddot{\gamma} = -\omega^2\gamma - 2\varepsilon\beta c\gamma^2.$$

These solutions satisfy

$$\mathrm{Re}\,\tilde{\sigma}_2 = 2\omega b\frac{2\lambda - 1}{3\lambda - 1}$$

(where $b = L(\tilde{\sigma})$ is time-dependent) and exist for all $\lambda \notin]0, \frac{1}{2}]$. As $\lambda \searrow \frac{1}{2}$ they turn into (33). We remark that these rectilinear solutions coincide with the rectilinear solutions $\tau_2 = (2\lambda - 1)/(3\lambda - 1)$ of the normal form, cf. (20).

This has implications for the transcritical bifurcation in the fourth-order normal form of the 2D Hénon–Heiles family we encountered in Section 4.5. Indeed, one would generically expect a transcritical bifurcation to break up into two centre–saddle bifurcations. However, this would lead to a small interval of λ-values with no equilibria on the upper arc. Thus, the

existence of rectilinear solutions of (1) forces the transcritical bifurcation to persist through all orders of the normal form of the 2D Hénon–Heiles family.

Directly solving the equations of motion allows us again to study these periodic orbits outside the range of validity of any normal form. For $\beta = 0$ the equatorial subsystem decouples and has rectilinear harmonic oscillations of all energies. The vertical oscillations (33) form a family that extends between the origin and the (un)stable manifold of the equilibrium $\sigma = (0, 0, (-\omega^3/\varepsilon\alpha))$. The family of rectilinear oscillations with direction $\theta \neq 0, \pi$ is bounded by the (un)stable manifold of

$$\sigma = \left(\frac{\omega^6}{2\beta^2\varepsilon^2} \left(1 - \frac{\alpha}{2\beta} \right), \frac{\omega^6}{2\beta^2\varepsilon^2} \left(1 - \frac{\alpha}{2\beta} \right), -\frac{\omega^3}{2\beta\varepsilon} \right).$$

Note that this latter equilibrium corresponds to a whole circle of equilibria in three degrees of freedom.

5.4. Reconstruction of the full system

We finally return to three degrees of freedom and reconstruct the dynamics of the full system X_{H_ε} on $T^*\mathbb{R}^3$. With the exception of $\{(0, 0, \sigma_3) | \sigma_3 \in \mathbb{C}\}$, every point of the reduced phase space $\{\sigma \in \mathbb{C}^3 | P(\sigma) = 0, \operatorname{Re}\sigma_2 \geq 0\}$ gets an S^1 attached. Where the Whittaker transformation (2) is defined, i.e. when $N \neq \pm G$, this S^1 is parametrised by the angle ν. The centres (36a,b) thereby turn into horizontal circular periodic orbits. Elliptic, hyperbolic and parabolic periodic orbits in $P^{-1}(0)$ become invariant 2-tori with the same normal behaviour. From invariant 2-tori with quasi-periodic motion we get invariant 3-tori that do not foliate into periodic orbits, but may be resonant. We collect below what we found out about the family (1) at non-exceptional ratios $\lambda = (\beta/\alpha)$ of the external parameters α, β in $\Lambda_1 :=]-1, 0[$, $\Lambda_2 :=]0, \frac{1}{2}[$, $\Lambda_3 :=]\frac{1}{2}, 1[$, $\Lambda_4 :=]1, \frac{5}{2}[$ or $\Lambda_5 :=]\frac{5}{2}, 6[\cup]6, \infty[\cup]-\infty, -1[$. When $\alpha = 0$ the behaviour of (1) is the same as for $\lambda \in \Lambda_5$.

Theorem 5.1. *Consider the Hamilton function* (1) *on* $T^*\mathbb{R}^3$. *For sufficiently small* ε *the corresponding flow has the following properties.*

A measure-theoretically large part of the phase space is filled by 3*D Cantor families of invariant* 3*-tori. On each energy shell the measure of their complement goes to zero as* $\varepsilon \to 0$. *The motion on these* 3*-tori is quasi-periodic with two or three independent frequencies. The Cantor families of invariant* 3*-tori shrink down to 2-parameter families of normally elliptic* 2*-tori. The horizontal circular periodic orbits reconstructed from* (36a,b) *are elliptic. The origin and occurring elliptic periodic orbits and normally elliptic invariant* 2*-tori are stable in the sense of Lyapunov.*

For $\lambda \in \Lambda_1$ *the stable and unstable manifolds of a 2-parameter family of normally hyperbolic invariant* 2*-tori separate the three Cantor families of invariant* 3*-tori. The periodic orbits restricted to the* (x_3, p_3) *subsystem are elliptic. The two families of normally elliptic invariant* 2*-tori that originate from these meet the family of normally hyperbolic* 2*-tori and vanish in (quasi-)periodic centre–saddle bifurcations.*

When $\lambda \in \Lambda_2$ *there are no normally hyperbolic invariant* 2*-tori. One of the 2-parameter families of normally elliptic invariant* 2*-tori originating from a family of horizontal circular*

periodic orbits extends to the other family of horizontal circular periodic orbits, while the other 2-parameter families of normally elliptic 2*-tori shrink down to the family of periodic orbits restricted to the* (x_3, p_3) *subsystem which are elliptic as well. The Cantor family of invariant* 3*-tori extends between the families of normally elliptic* 2*-tori.*

The situation for $\lambda \in \Lambda_3$ *is similar to that of* $\lambda \in \Lambda_2$ *except that the periodic orbits restricted to the* (x_3, p_3) *subsystem are now hyperbolic. Within the invariant submanifold* $N = 0$ *their stable and unstable manifolds separate two Cantor families of invariant* 3*-tori which shrink down to the two families of normally elliptic* 2*-tori.*

For $\lambda \in \Lambda_4$ *there are two Cantor families of invariant* 3*-tori, which are separated by the stable and unstable manifolds of a 2-parameter family of normally hyperbolic invariant* 2*-tori. These undergo (quasi-)periodic Hamiltonian flip bifurcations and become normally elliptic, shrinking down to the horizontal circular periodic orbits. The second family of normally elliptic* 2*-tori originating from the latter extend to the periodic orbits restricted to the* (x_3, p_3) *subsystem which are elliptic as well.*

The situation for $\lambda \in \Lambda_5$ *is similar to that of* $\lambda \in \Lambda_4$ *except that the periodic orbits restricted to the* (x_3, p_3) *subsystem are now hyperbolic. Within the invariant submanifold* $N = 0$ *there are three Cantor families of invariant* 3*-tori. Two of these shrink down to the normally elliptic* 2*-tori, and one Cantor family extends between the stable/unstable manifolds of the hyperbolic periodic orbits and the normally hyperbolic invariant* 2*-tori.*

For $\lambda \in \Lambda_1$ *the normally hyperbolic invariant* 2*-tori within* $\{N = 0\}$ *consist of rectilinear solutions. In case* $\lambda \in \Lambda_3 \cup \Lambda_4 \cup \Lambda_5$ *this holds true for the normally elliptic invariant* 2*-tori within* $\{N = 0\}$ *with minimal energy.*

We end with a discussion of the exceptional values $-1, 0, \frac{1}{2}, 1, \frac{5}{2}, 6$ of the ratio $\lambda = \beta/\alpha$. Here not only the behaviour of (1) for such a fixed value λ is of interest, but also how the behaviour changes as λ is varied and passes through one of these values.

Theorem 5.2. *Consider the Hamilton function* (1) *on* $T^*\mathbb{R}^3$. *Sufficiently close to the origin there is a critical interval* $]\lambda_*, 6[$ *of ratios* $\lambda = \beta/\alpha$ *for which the situation is similar to that of* $\lambda \in \Lambda_5$ *except for the following.*

The horizontal circular periodic orbits reconstructed from (36a,b), *which are parametrised by the value a of N, have a normal behaviour in* 2–1 *resonance for* $a = \pm A(\lambda)$. *As a passes through these two values, the (quasi-)periodic Hamiltonian flip bifurcation approaches the almost circular equatorial periodic orbits, reaches them when* $|a| = A(\lambda)$, *and withdraws again after the passage through* $\pm A(\lambda)$.

For the normal form $\bar{H}_\varepsilon$ of order 2 the periodic orbit restricted to the (x_3, p_3) subsystem changes its behaviour when $\alpha = 2\beta$ or $5\alpha = 2\beta$. This implies that there are critical ratios λ_* and λ^* of (β/α) close to $\frac{1}{2}$ and $\frac{5}{2}$ where the vertical oscillations (33) bifurcate. In Section 5.3 we have seen that in fact $\lambda_* = \frac{1}{2}$, and the results in [8] suggest that $\lambda^* = \frac{5}{2}$ as well. We conjecture that a (periodic) Hamiltonian Hopf bifurcation of hyperbolic type occurs as (β/α) passes through these exceptional values. Note that τ_4 only enters squared in (19), through $\tau_5 = \tau_2^2 - \tau_4^2$. Correspondingly, there is a fourfold zero eigenvalue at the bifurcation. We refer to [31] for further details.

In the exceptional cases $\alpha = \beta$ and $\beta = 0$ the Hamiltonian system defined by (1) is integrable. We have seen in Section 4.5 that this leads to degenerate normal forms. As β passes through 0 a degenerate bifurcation takes place in the normal form. For $N = 0$, i.e. for the 2D Hénon–Heiles family, it has been shown in [32] that this degenerate bifurcation occurs in the original system as well. We expect that the same techniques allow for this same conclusion in the family (1).

For $\alpha = \beta$ the flow defined by the normal form is very degenerate, having a 3-parameter family of invariant 2-tori. Note that this case separates the quite different dynamical behaviours of $(\beta/\alpha) \in \Lambda_3$ and $(\beta/\alpha) \in \Lambda_4$.

The case $\alpha = -\beta$ is the 3D Hénon–Heiles system and has been studied in [21,22,58]. Here the degeneracy of the second-order normal form is broken by the fourth-order normal form. To understand the changes in the behaviour of the system defined by (1) as (β/α) varies near $\lambda = -1$ it would be instructive to study the fourth-order normal form for a range of parameter values around $\alpha = -\beta$. For instance, we expect connection bifurcations as in [8] to occur.

As remarked in Section 1 there is one more case, $\alpha = 6\beta$, where (1) defines an integrable system. Hence, the Cantor family of invariant 3-tori becomes a smooth 3-parameter family. But there are no effects of the integrability on invariant 2-tori or periodic orbits. The second-order normal form (19) is independent of τ_1 if $\alpha = 6\beta$. As shown in [19] the higher order normal forms break this symmetry.

6. Conclusions

In the present paper we studied the 3D Hénon–Heiles family (1) with sufficiently small ε. For most values of $\lambda = (\beta/\alpha)$ we could describe the phase flow, which is governed by the normal form of order 2. In condensed form the pertinent information is contained in the set Σ of singular values of the energy–momentum mapping. For the six generic cases Σ is depicted in Fig. 5, see also Fig. 3.

Furthermore we laid the foundations for further study of the behaviour as λ varies near the exceptional values $-1, 0, \frac{1}{2}, 1, \frac{5}{2}, 6$ which separate the generic cases. For these special values the set Σ of singular values of the energy–momentum mapping is given in Fig. 6. We conjecture that Hamiltonian Hopf bifurcations take place at the values $\frac{1}{2}, \frac{5}{2}$ of λ. We did not address the monodromy in the normal form as it will be a consequence of occurring Hamiltonian Hopf bifurcations.

The normalisation was performed in various forms. It turned out that the variables (3) performed best. However, this may be conceptually more involved since the Poisson structure, given in Table 1, is non-standard.

The symmetry reduction by means of invariants seems to be the proper tool. They provide a global description of the reduced phase space. The nodal-Lissajous variables allow for an intuitive understanding of the fibres $S^1 \times S^1$. Where they are defined they trivialise the bundle $T^*\mathbb{R}^3$.

While the local co-ordinates (γ, Γ) on the reduced phase space, which are derived from the nodal-Lissajous variables, favour a description in terms of the "plane of motion" of the unperturbed oscillator, the invariants τ_1, τ_2 favour a description in terms of "equatorial versus vertical". In this way one has two complementary interpretations of the points on the

reduced phase space. For $a \neq 0$ there is a singularity at $\Gamma = \frac{1}{2}|a|$ which can be regularised by passing to a 2:1 cover of the reduced phase space. The nodal-Lissajous variables g and G are polar-like co-ordinates around the "desingularised" point.

In principle all computations can be done in nodal-Lissajous variables as well, except on the upper arc $G = 0$ of the lemon $a = 0$. Here (1) reduces (fixing the angle ν) to the 2D Hénon–Heiles family and one may use the Lissajous variables of [15]. In some cases this even leads to simpler formulae. However, in this way one misses geometric insight concerning the dynamical behaviour close to $G = 0$.

The adequate use of a symbolic manipulator has been essential to achieve some conclusions along the paper; for example, to carry out the normal form computations and to determine the stability of periodic orbits and invariant 2-torus.

We encountered centre–saddle and Hamiltonian flip bifurcations. The former occur at regular points of the twice reduced phase space and had already been dealt with in [12]. In a Hamiltonian flip bifurcation of the normal form the singular point $\tau = (0, 1)$ of the twice reduced phase space V_μ changes its normal behaviour. To avoid the technicalities of singularity theory on non-smooth phase spaces, we regularised that point by passing to a 2:1 cover U_μ of V_μ. In this way the Hamiltonian flip bifurcation turned into a Hamiltonian pitchfork bifurcation. We remark that the pertinent transversality conditions, $\gamma_i \neq 0$ in (27), have immediate geometric interpretations concerning the relative positions (within $\mathbb{R}^3$) of V_μ and the level set $\{\mathcal{H}^\lambda = h\}$.

As λ passes through $\frac{1}{2}$, $\frac{5}{2}$ the singular point $\tau = (0, 0)$ bifurcates and the relative positions of V_0 and $\{\mathcal{H}^\lambda = h\}$ fulfill these same geometric transversality conditions. This is used in [31] to prove that indeed a Hamiltonian Hopf bifurcation takes place.

It would be helpful to have a ready-to-apply theory of deformations and unfoldings on singular spaces. For a first step in this direction see [53], and see [39] for the theoretical groundwork that seems necessary for further progress.

In Section 5.3 of [24] the Hamilton function

$$K_\varepsilon = H_0 + \varepsilon xyz + \frac{\varepsilon^2}{2\omega^2}\left(x^4 + \frac{23}{9}x^2y^2 + y^4 + z^4\right)$$

is introduced as an example of a perturbation of H_0 that is not axially symmetric, but has an axially symmetric normal form $\bar{K}_\varepsilon$ of order 2. Adding $K_\varepsilon - \bar{K}_\varepsilon$ to (1) we obtain a family of Hamiltonian systems that are *not* axially symmetric, but have the same (axially symmetric) normal form of order 2 (17) as (1). In particular, all results obtained in Section 4 remain valid.

However, the perturbation analysis of Section 5.2 does not apply any more. Instead, the perturbation analysis has to be carried out in three degrees of freedom, with KAM-like arguments replacing the use of the implicit mapping theorem. As an intermediate step, one could study on $\mathbb{CP}^2$ how the normal form of order 4 breaks the axial symmetry and only then look at the full dynamics in three degrees of freedom.

While this particular example $H_\varepsilon + K_\varepsilon - \bar{K}_\varepsilon$ is a bit constructed, this shows how the understanding of axially symmetric perturbations may help to analyse the whole unfolding of the 1–1–1 resonance.

Acknowledgements

We thank Sang-Woo Cho and Juan Félix San Juan for their help in the normal form computations. We also are indebted to Richard Cushman and the anonymous referee for their valuable comments. The figures were made using the software packages ESFERAS and Mathematica, see [49,57] for descriptions. Partial support for this research was given by the Comisión Interministerial Científica y Técnica of Spain (CICYT PB 95-0795), by a Project of Departamento de Educación y Cultura, Gobierno de Navarra, Orden Foral 508/1997 (Spain), Ayuda de Formación de Profesorado de la Universidad Pública de Navarra, by the Ministerio de Educación y Cultura of Spain (PB 98-1576) and by the Graduiertenkolleg Analyse und Konstruktion in der Mathematik.

References

[1] R. Abraham, J.E. Marsden, Foundations of Mechanics, 2nd Edition, Benjamin, New York, 1978.
[2] Y. Aizawa, N. Saitô, On the stability of isolating integrals. I. Effect of the perturbation in the potential function, J. Phys. Soc. Jpn. 32 (1972) 1636–1640.
[3] V.I. Arnol'd, Small denominators and problems of stability of motion in classical and celestial mechanics, Russ. Math. Surv. 18 (6) (1963) 85–191.
[4] V.I. Arnol'd, Mathematical Methods of Classical Mechanics, Springer, Berlin, 1978.
[5] H.W. Broer, G.B. Huitema, A proof of the isoenergetic KAM-theorem from the ordinary one, J. Diff. Eq. 90 (1) (1991) 52–60.
[6] H.W. Broer, G.B. Huitema, M.B. Sevryuk, Quasi-periodic Motions in Families of Dynamical Systems Order Amidst Chaos, Lecture Notes in Mathematics, Vol. 1645, Springer, Berlin, 1996.
[7] H.W. Broer, G. Vegter, Bifurcational aspects of parametric resonance, Dyn. Rep. New Ser. 1 (1992) 1–53.
[8] C. Cotter, The 1:1 semisimple resonance, Ph.D. Thesis, University of California, Santa Cruz, 1986.
[9] D. Cox, J. Little, D. O'Shea, Ideals, Varieties and Algorithms: An Introduction to Computational Algebraic Geometry and Commutative Algebra, Springer, Berlin, 1992.
[10] R. Cushman, Geometry of the bifurcations of the normalized reduced Hénon–Heiles family, Proc. R. Soc. London A 382 (1982) 361–371.
[11] R. Cushman, L.M. Bates, Global Aspects of Classical Integrable Systems, Birkhauser, Basel, 1997.
[12] R. Cushman, S. Ferrer, H. Hanßmann, Singular reduction of axially symmetric perturbations of the isotropic harmonic oscillator, Nonlinearity 12 (1999) 389–410.
[13] A. Deprit, Canonical transformations depending on a small parameter, Celes. Mech. 1 (1969) 12–30.
[14] A. Deprit, The elimination of the parallax in satellite theory, Celes. Mech. 24 (1981) 111–153 .
[15] A. Deprit, The Lissajous transformation — I. Basics, Celes. Mech. Dyn. Astron. 51 (1991) 201–225.
[16] A. Deprit, A. Elipe, The Lissajous transformation — II. Normalization, Celes. Mech. Dyn. Astron. 51 (1991) 227–250.
[17] J.J. Duistermaat, Non-integrability of the 1:1:2-resonance, Ergod. Theory Dyn. Syst. 4 (1984) 553–568.
[18] J.J. Duistermaat, The monodromy of the Hamiltonian Hopf bifurcation, Z. Angew. Math. Phys. 49 (1998) 156–161.
[19] D. Farrelly, J. Humpherys, T. Uzer, Normalization of resonant Hamiltonians, in: J. Seimenis (Ed.), Hamiltonian Mechanics, Integrability and Chaotic Behavior, Torun 1993, Plenum Press, New York, 1994, pp. 237–244.
[20] S. Ferrer, A. Gárate, On perturbed 3D elliptic oscillators: a case of critical inclination in galactic dynamics, in: E.A. Lacomba, J. Llibre (Eds.), New Trends for Hamiltonian Systems and Celestial Mechanics, Cocoyoc 1994, Advanced Series in Nonlinear Dynamics, Vol. 8, World Scientific, Singapore, 1996, pp. 179–197.
[21] S. Ferrer, M. Lara, J. Palacián, J.F. San Juan, A. Viartola, P. Yanguas, The Hénon and Heiles problem in three dimensions. I. Periodic orbits near the origin, Int. J. Bifurc. Chaos Appl. Sci. Eng. 8 (1998) 1199–1213.

[22] S. Ferrer, M. Lara, J. Palacián, J.F. San Juan, A. Viartola, P. Yanguas, The Hénon and Heiles problem in three dimensions. II. Relative equilibria and bifurcations in the reduced system, Int. J. Bifurc. Chaos Appl. Sci. Eng. 8 (1998) 1215–1229.
[23] S. Ferrer, M. Lara, J. Palacián, P. Yanguas, On perturbed oscillators in 1–1–1 resonance: critical inclination in the 3D Hénon–Heiles potential, in: C. Simó (Ed.), Hamiltonian Systems with Three or More Degrees of Freedom, S'Agaró, 1995, Kluwer Academic Publishers, Dordrecht, The Netherlands, 1999, pp. 362–366.
[24] S. Ferrer, J. Palacián, P. Yanguas, Hamiltonian oscillators in 1–1–1 resonance: normalization and integrability, J. Nonlinear Sci. 10 (2000) 145–174.
[25] D.M. Fradkin, Three-dimensional isotropic harmonic oscillator and SU_3, Am. J. Phys. A 33 (1965) 207–211.
[26] W. Gröbner, Die Lie–Reihen und ihre Anwendungen, Verlag der Wissenschaften, Berlin, 1967.
[27] M.C. Gutzwiller, Chaos in Classical and Quantum Mechanics: Interdisciplinary Applied Mathematics, Vol. 1, Springer, New York, 1990.
[28] G. Haller, S. Wiggins, Geometry and chaos near resonant equilibria of 3-DOF Hamiltonian systems, Physica D 90 (1996) 319–365.
[29] H. Hanßmann, Quasi-periodic motions of a rigid body — a case study on perturbations of superintegrable systems, Ph.D. Thesis, Rijksuniversiteit Groningen, 1995.
[30] H. Hanßmann, Equivariant perturbations of the Euler top, in: H.W. Broer, et al. (Eds.), Nonlinear Dynamical Systems and Chaos, Groningen, 1995, Progress in Nonlinear Differential Equations and Their Applications, Vol. 19, Birkhauser, Basel, 1996, pp. 227–252.
[31] H. Hanßmann, J.-C. van der Meer, On the Hamiltonian Hopf bifurcations in the 3D Hénon–Heiles family, in preparation.
[32] H. Hanßmann, B. Sommer, A degenerate bifurcation in the Hénon–Heiles family, Inst. Reine and Angew. Math., RWTH Aachen, Preprint, 2000.
[33] M. Hénon, C. Heiles, The applicability of the third integral of motion: some numerical experiments, Astron. J. 69 (1964) 73–79.
[34] A. Holas, N.H. March, A generalisation of the Runge–Lenz constant of classical motion in a central potential, J. Phys. A 23 (1990) 735–749.
[35] I. Hoveijn, Aspects of resonance in dynamical systems, Ph.D. Thesis, Universiteit Utrecht, 1993.
[36] J.M. Jauch, E.L. Hill, On the problem of degeneracy in quantum mechanics, Phys. Rev. 57 (1940) 641–645.
[37] M. Kummer, On resonant classical Hamiltonians with n frequencies, J. Diff. Eq. 83 (1990) 220–243.
[38] M. Lakshmanan, R. Sahadevan, Painlevé analysis, Lie symmetries, and integrability of coupled nonlinear oscillators of polynomial type, Phys. Rep. 224 (1993) 1–93.
[39] G.A. Lunter, Bifurcations of Hamiltonian systems — computing singularities by Gröbner bases, Ph.D. Thesis, Rijksuniversiteit Groningen, 1999.
[40] G. Marmo, E.J. Saletan, A. Simoni, B. Vitale, Dynamical Systems — A Differential Geometric Approach to Symmetry and Reduction, Wiley, New York, 1985.
[41] M. Mazzocco, KAM theorem for generic analytic perturbations of the Euler system, Z. Angew. Math. Phys. 48 (1997) 193–219.
[42] J.-C. van der Meer, The Hamiltonian Hopf bifurcation, Lecture Notes in Mathematics, Vol. 1160, Springer, Berlin, 1985.
[43] K.R. Meyer, Generic bifurcation of periodic points, Trans. AMS 149 (1970) 95–107.
[44] K.R. Meyer, Normal forms for the general equilibrium, Funkcial. Ekva. 27 (1984) 261–271.
[45] B.R. Miller, The Lissajous transformation — III. Parametric bifurcations, Celes. Mech. Dyn. Astron. 51 (1991) 251–270.
[46] J. Moser, Regularization of Kepler's problem and the averaging method on a manifold, Commun. Pure Appl. Math. 23 (1970) 609–636.
[47] N.N. Nehorošev, Action–angle variables and their generalizations, Trans. Mosc. Math. Soc. 26 (1972) 180–198.
[48] T.Z. Nguyen, A note on focus–focus singularities, Diff. Geom. Appl. 7 (2) (1997) 123–130.
[49] P. Pascua, J.L. Rubio, A. Viartola, S. Ferrer, Visualizing relative equilibria and bifurcations by painting Hamiltonians on personal computers, Int. J. Bifurc. Chaos Appl. Sci. Eng. 6 (1996) 1411–1424.
[50] A. Ramani, B. Grammaticos, T. Bountis, The Painlevé property and singularity analysis of integrable and non-integrable systems, Phys. Rep. 180 (1989) 159–245.

[51] A.F. Saaf, A formal third integral of motion in a nearly spherical stellar system, Astrophys. J. 154 (1968) 483–498.
[52] J.A. Sanders, F. Verhulst, Averaging Methods in Nonlinear Dynamical Systems, Springer, Berlin, 1985.
[53] D. Siersma, Singularities of functions on boundaries, corners, etc., Quart. J. Math. Oxford 32 (2) (1981) 119–127.
[54] B. Sommer, Über eine Bifurkation der Hénon–Heiles-Familie, Diplomarbeit, RWTH Aachen, 1997.
[55] F. Verhulst, Discrete symmetric dynamical systems at the main resonances with applications to axi-symmetric galaxies, Phil. Trans. R. Soc. London A 290 (1979) 435–465.
[56] E.T. Whittaker, A Treatise on the Analytical Dynamics of Particles and Rigid Bodies, Cambridge University Press, Cambridge, 1904.
[57] S. Wolfram, The Mathematica Book, 3rd Edition, Wolfram Media/Cambridge University Press, Cambridge, 1996.
[58] P. Yanguas, Integrability, normalization and symmetries of Hamiltonian systems in 1–1–1 resonance, Ph.D. Thesis, Universidad Pública de Navarra, 1998.
[59] T. de Zeeuw, Motion in the core of a triaxial potential, Mon. Not. R. Astron. Soc. 215 (1985) 731–760.
[60] T. de Zeeuw, Dynamical models for axisymmetric and triaxial galaxies, in: T. de Zeeuw, (Ed.), Structure and Dynamics of Elliptical Galaxies, IAU Symp., Vol. 127, Reidel, Dordrecht, 1987, pp. 271–290.
[61] T. de Zeeuw, M. Franx, Structure and dynamics of elliptical galaxies, Annu. Rev. Astron. Astrophys. 29 (1991) 239–274.
[62] T. de Zeeuw, D. Merritt, Stellar orbits in a triaxial galaxy. I. Orbits in the plane of rotation, Astrophys. J. 267 (1983) 571–595.